Diffuse Lung Disease

R. Paul Guillerman

Contents

Abstract

Diffuse lung disease (DLD) comprises a diverse group of disorders characterized by widespread pulmonary parenchymal pathology and impaired gas exchange. While many of these disorders are categorized under the rubric of interstitial lung disease (ILD), some of these disorders involve the airspaces or peripheral airways in addition to, or rather than, the interstitium. Some of these disorders are present primarily in infancy or early childhood, while others that are prevalent in adulthood rarely occur in childhood. This chapter will review the classification of pediatric DLD and the characteristic imaging findings of specific disorders to facilitate accurate diagnosis and guide appropriate treatment of children with these disorders.

1 Introduction

Diffuse lung disease (DLD) comprises a diverse group of disorders characterized by widespread pulmonary parenchymal pathology and impaired gas exchange. While many of these disorders in children are categorized under the rubric of interstitial lung disease (ILD), some of these disorders involve the airspaces or peripheral airways in addition to, or rather than, the interstitium, so that DLD is a less specific, but more inclusive term. The American Thoracic Society (ATS) /European Respiratory Society (ERS) international multidisciplinary classification of the idiopathic interstitial pneumonias (Travis et al. 2013) developed for the adult population is not well suited for children.

Many of the disorders that are most prevalent in adulthood rarely occur in childhood. Usual interstitial pneumonia (UIP), the pathologic correlate of idiopathic pulmonary fibrosis (IPF) and the predominant form of DLD in the adult ATS/ERS classification, is exceedingly rare in children and erroneous diagnoses likely account for reports of better

R. P. Guillerman (✉)
Department of Pediatric Radiology, Texas Children's Hospital, Baylor College of Medicine, Houston, TX, USA
e-mail: rpguille@texaschildrens.org

P. Garcia-Peña and R. P. Guillerman (eds.), *Pediatric Chest Imaging*, Medical Radiology. Diagnostic Imaging,
DOI: 10.1007/174_2014_1021, © Springer-Verlag Berlin Heidelberg 2014
Published Online: 1 June 2014

outcomes of children with UIP compared to adults. Unrecognized mutations in surfactant-related genes likely account for many reported cases of desquamative interstitial pneumonia (DIP) in children diagnosed before the availability of tests for these mutations (Fan et al. 2004; Nogee 2006).

There are several types of DLD that present primarily or exclusively in infancy or early childhood, such as neuroendocrine cell hyperplasia of infancy (NEHI) and pulmonary interstitial glycogenosis (PIG). The stage of lung growth and development affects disease manifestations, and the injury and repair processes in immature lung differ from those in the mature adult lung (Clement and Eber 2008). In recognition of these differences with adult DLD, standardized approaches to the diagnosis and classification of pediatric DLD have been advocated, incorporating insights from diagnostic imaging, infant pulmonary function testing, molecular genetics, immunopathology, and electron microscopy (Deutsch et al. 2007). This chapter will review the classification, clinical features, and imaging findings of pediatric DLD.

2 Clinical Presentations and Classification

DLD is less prevalent in children than in adults and more common in infants than in older children. While rare, the true prevalence of pediatric DLD is likely understated in the medical literature as a consequence of more hesitant use of diagnostic lung biopsy in children compared to adults and the lack of familiarity with recently described disorders and appropriate classification.

Pediatric DLD usually presents either with rapid respiratory failure in the neonatal period or with an insidious course of respiratory signs and symptoms, failure to thrive, or exercise intolerance later in infancy, childhood, or adolescence. The signs and symptoms may be misattributed for many months or even years to common disorders, such as pulmonary infection, bronchopulmonary dysplasia (BPD), asthma, congenital heart disease, cystic fibrosis, or immunodeficiency. Once these common disorders have been eliminated as causal, criteria have been devised to assist clinicians in identifying children that warrant further investigation for possible DLD. A neonate or infant is proposed as having "childhood ILD syndrome" or "chILD syndrome" if at least three of the following criteria are present: (1) respiratory symptoms (cough, rapid, and/or difficult breathing, or exercise intolerance), (2) signs (tachypnea, adventitious sounds, retractions, digital clubbing, failure to thrive, or respiratory failure), (3) hypoxemia; and (4) diffuse pulmonary parenchymal abnormality on chest radiograph (CXR) or computed tomography (CT) (Kurland et al. 2013).

Correct diagnosis of a DLD is important due to widely differing prognoses among the disorders and the need for genetic evaluation and counseling for some families. To promote effective communication for clinical care and research, the disorders affecting infants and young children with "chILD syndrome" have been organized by the chILD Research Cooperative into a novel classification scheme (Deutsch et al. 2007) categorized on the basis of the presumed etiology, with overlap of distinct clinical disorders and pathologies among different etiologic categories. For example, pulmonary alveolar proteinosis (PAP), DIP, nonspecific interstitial pneumonia (NSIP), and chronic pneumonitis of infancy (CPI) are distinct pathologies that can be associated with genetic surfactant disorders, and NSIP pathology can be observed in genetic disorders of surfactant metabolism, disorders related to systemic disease processes (such as immune-mediated connective tissue disease) or disorders of the normal immunocompetent host (such as hypersensitivity pneumonitis). In such a classification based on etiology, disorders that can be idiopathic or secondary to other conditions are difficult to categorize. Despite its limitations, the chILD classification scheme has been found applicable to over 90 % of cases of DLD encountered in the setting of a children's hospital, including previously unclassified cases (Soares et al. 2013), and several of the disorders are recognized by diagnosis codes in the latest versions of the International Classification of Diseases by the World Health Organization (Popler et al. 2012). While the chILD classification generally works well for infants and young children (Langston and Dishop 2009), expansion and modification of the classification is necessary for older children and adolescents who may manifest with forms of DLD more prevalent in adults (Rice et al. 2013) (Table 1). Infants are more likely to have developmental, growth, or genetic disorders, while older children and adolescents are more likely to have disorders related to systemic diseases, infections, or environmental exposures.

The imaging technique and diagnostic efficacy of imaging for pediatric DLD have been addressed in previous review articles (Guillerman 2010; Guillerman and Brody 2011; Lee 2013). For some types of pediatric DLD, the imaging findings are highly specific, while for others the imaging findings are nonspecific and laboratory tests or lung biopsy are needed for definitive diagnosis (Kurland et al. 2013). In addition to suggesting or corroborating a specific diagnosis in some cases, imaging can be useful for refining the differential diagnosis, identifying biopsy sites, monitoring disease activity, and assessing response to therapy. The remainder of this chapter will provide an updated summary of the characteristic clinical and imaging features of the disorders categorized under a modified chILD classification scheme of pediatric DLD.

Table 1 Classification scheme for pediatric diffuse lung disease

Disorders more prevalent in infants and young children
Diffuse developmental disorders
Acinar dysplasia
Congenital alveolar dysplasia
Alveolar capillary dysplasia with misalignment of the pulmonary veins
Growth abnormalities
Pulmonary hypoplasia
Chronic lung disease of infancy
Related to genetic disorders
Related to congenital heart disease
Specific disorders of unknown etiology
Pulmonary interstitial glycogenosis
Neuroendocrine cell hyperplasia of infancy
Surfactant dysfunction disorders
Related to a genetic defect
Related to autoimmune anti-GM-CSF antibody
Consistent histology without a recognized genetic defect
Disorders related to systemic disease processes
Autoimmune and autoinflammatory disorders
Vasculitis
Connective tissue disease
Immunodeficiencies
Primary
Secondary (drug therapy, radiation therapy, bone marrow transplant)
Lymphoid hyperplasia and lymphoproliferative disorders
Granulomatous disorders
Lysosomal storage disorders
Langerhans cell histiocytosis
Disorders of the normal immunocompetent host
Infectious and post-infectious processes
Bronchiolitis obliterans
Eosinophilic pneumonia
Related to exposures
Hypersensitivity pneumonitis
Aspiration pneumonia
Drug reaction
Toxic inhalation
Acute interstitial pneumonia
Cryptogenic organizing pneumonia
Idiopathic nonspecific interstitial pneumonia
Idiopathic pulmonary hemosiderosis
Vascular disorders masquerading as diffuse lung disease
Pulmonary venous congestion or obstruction
Congestive heart failure
Congenital cardiovascular disease
Pulmonary veno-occlusive disease
Lymphangiectasia
Lymphangiomatosis

[adapted from Deutsch et al. (2007) and Rice et al. (2013)]

3 Categories of Disorders

3.1 Diffuse Developmental Disorders

Acinar dysplasia is characterized by lung developmental arrest in the pseudoglandular or early canalicular phase, resulting in essentially no alveolar spaces for gas exchange. Congenital alveolar dysplasia is characterized by arrest in the late canalicular/early saccular phase, resulting in incomplete alveolarization. Alveolar capillary dysplasia with misalignment of the pulmonary veins (ACD/MPV) is characterized by malpositioning of the pulmonary vein branches adjacent to the pulmonary artery branches rather than within the interlobular septa, medial hypertrophy of the pulmonary arterioles, reduced alveolar capillary density, and pulmonary lobular maldevelopment. Pulmonary lymphangiectasia is also present in about one-third of cases (Dishop 2011). The misaligned pulmonary veins in ACD/MPV may actually represent anastomotic bronchial veins associated with intrapulmonary right-to-left shunting. This shunting bypasses the alveolar capillary bed and exacerbates the hypoxemia from right-to-left extrapulmonary shunting associated with persistent pulmonary hypertension of the newborn (PPHN) (Galambos et al. 2014).

The diffuse developmental disorders of the lung are associated with markedly impaired alveolar gas exchange, resulting in respiratory failure and severe PPHN within hours or days of birth in the absence of the usual causative conditions of prematurity, meconium aspiration, congenital heart disease, perinatal asphyxia, or sepsis. Death usually ensues within a few days or weeks, unless the lung involvement is patchy rather than diffuse (Chow et al. 2013), or extracorporeal membrane oxygenation (ECMO) or paracorporeal lung assist devices are available as a bridge to lung transplantation (Sen et al. 2004; Michalsky et al. 2005; Hoganson et al. 2014). Approximately 80 % of cases of ACD/MPV are associated with extrapulmonary malformations, including hypoplastic left heart syndrome, aortic coarctation, alimentary tract atresia, annular pancreas, omphalocele, midgut malrotation, and urinary tract malformation. Sporadic or familial autosomal dominant *FOXF1* gene mutations have been identified as a cause of some cases of ACD/MPV (Stankiewicz et al. 2009; Sen et al. 2013).

Due the severity of the respiratory disease, imaging of patients with diffuse developmental disorders of the lung is usually limited to portable CXRs. Although the initial CXRs may be unimpressive, followup CXRs may demonstrate progressive hazy opacification of the lungs, resembling of the findings of surfactant deficiency of prematurity or genetic surfactant disorders (Fig. 1). Pneumothorax or pneumomediastinum is common and likely attributable to barotrauma (Michalsky et al. 2005; Hugosson et al. 2005; Gillespie et al. 2004; Newman and Yunis 1990).

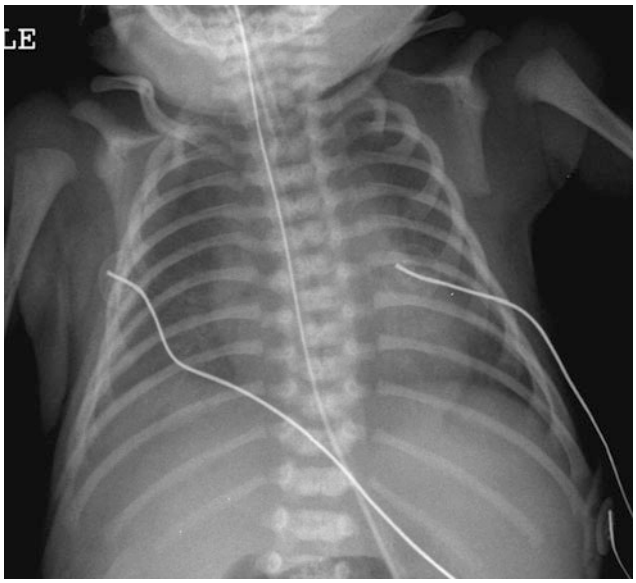

Fig. 1 Alveolar capillary dysplasia with misalignment of the pulmonary veins (ACD/MPV). A frontal portable CXR of a 33-week gestational age newborn with neonatal RDS shows diffuse, hazy pulmonary opacification indistinguishable from surfactant deficiency of prematurity. The patient rapidly developed hypoxemia and severe PPHN requiring ECMO

3.2 Growth Abnormalities

Growth abnormalities constitute the most common cause of chronic DLD in infancy. Lung growth abnormalities are characterized histologically by impaired alveolarization manifesting as lobular simplification with deficient alveolar vascularization and septation, reduced alveolar number, and increased alveolar size resembling emphysema (Dishop 2010). As a consequence, there is diminished total alveolar surface area and reduced pulmonary diffusing capacity relative to alveolar volume (Balinotti et al. 2010). Lung growth abnormalities are often accompanied by patchy PIG or by pulmonary arterial hypertensive changes related to increased vascular resistance from a deficient capillary bed (Dishop 2011).

Lung growth abnormalities can be related to prenatal or postnatal conditions (Deutsch et al. 2007). The most common prenatal form is pulmonary hypoplasia secondary to limited intrathoracic space in utero, such as from a congenital diaphragmatic hernia, oligohydramnios, thoracic mass lesion, or skeletal dysplasia. The most frequently encountered postnatal form is chronic lung disease of infancy (CLDI) related to prematurity. This includes "new" BPD, which is characterized by impaired alveolarization, but less fibrosis and airway obstruction compared to classic BPD (Bhandari and Bhandari 2009), and Wilson-Mikity syndrome, which is characterized by slowly progressive respiratory distress and cyst-like changes of the lungs developing within the first few weeks of life despite minimal respiratory support at birth (Hoepker et al. 2008; Philip 2009). Growth abnormalities can also be observed in near-term and term infants as an idiopathic disorder or in association with congenital heart disease or certain genetic disorders (Deutsch et al. 2007; Dishop 2010).

Patients with a lung growth abnormality typically present with respiratory difficulty as a neonate, and may either improve or worsen, depending on the extent of catch-up growth of the alveoli over time and whether or not pulmonary hypertension ensues. Most alveolarization occurs by two to three years postnatal age, but recent evidence from hyperpolarized gas magnetic resonance imaging suggests that neo-alveolarization continues to occur throughout childhood and adolescence in normal individuals (Narayanan et al. 2012). Gestational age at birth is an important determinant of subsequent alveolar development (Balinotti et al. 2010), but the capacity for catch-up neo-alveolarization in those with lung growth abnormalities is currently unknown.

The chest imaging findings of infants with BPD and other lung growth abnormalities range from nearly normal to markedly abnormal, with distorted pulmonary lobules of variable shape and attenuation, perilobular reticular opacities, linear subpleural opacities, ground-glass opacities, and foci of decreased lung attenuation, often appearing as cyst-like hyperlucencies (Metwalli et al. 2011) (Fig. 2). The decreased lung attenuation is likely attributable to enlarged alveoli with reduced alveolar septation and vascularization (Mahut et al. 2007). Decreased lung attenuation on CT correlates with the clinical severity of BPD (la Tour et al. 2013). Reproducible quantitative CT scoring systems based on the extent of findings, such as decreased lung attenuation, linear opacities, and architectural distortion at a mean postmenstrual age of 39 weeks show better correlation than do CXR scores with the clinical severity of BPD, and higher CT scores predict a higher risk of rehospitalization for pneumonia (Shin et al. 2013). CT scoring systems are superior to pulmonary function testing for differentiating infants with and without a history of BPD and higher CT scores are associated with a greater number of days on supplemental oxygen (Sarria et al. 2011). Ventilation-perfusion (V/Q) single photon emission computed tomography (SPECT) performed at a mean postmenstrual age of 37 weeks commonly reveals V/Q mismatching, even in clinically mild BPD, and the degree of V/Q mismatching correlates with the duration of mechanical ventilation (Kjellberg et al. 2013). Residual pulmonary abnormalities on CT are very common in adolescent and young adult survivors of classic BPD born in the pre-surfactant era, with the most frequent findings being subpleural, triangular, and linear opacities, air trapping, and emphysema (Aukland et al. 2006; Wong et al. 2008, 2011) (Fig. 3). The imaging findings in adolescent and adult survivors of "new" BPD

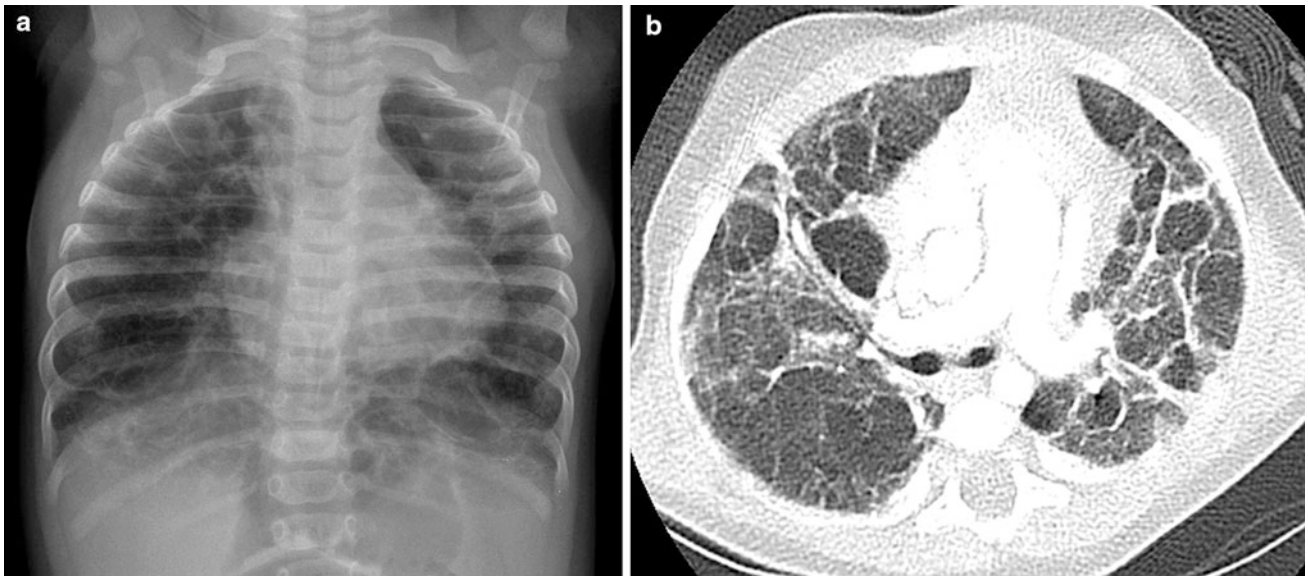

Fig. 2 Growth abnormality. A frontal CXR (**a**) of a five-month-old, former 32-week preemie with CLDI and continued supplemental oxygen requirement shows pulmonary hyperinflation, reticular opacities, and cystic changes. An axial chest CT image (**b**) demonstrates architectural distortion with ground-glass opacities, thick perilobular opacities, and variably-sized pulmonary lobules, some of which exhibit cyst-like hyperlucency related to alveolar simplification

are not yet well described. The imaging findings of BPD are further discussed in the chapter entitled Neonatal Chest Imaging by Crotty in this book.

Down syndrome is associated with a peculiar lung growth abnormality in which the enlargement of the alveoli and alveolar ducts is particularly marked in the subpleural region, resulting in the appearance of subpleural cysts on CT (Biko et al. 2008) (Fig. 4). A lung growth abnormality should be suspected in children with Down syndrome and respiratory difficulties not attributable to congenital heart disease.

A severe progressive lung growth disorder ultimately requiring lung transplantation for survival can develop in infants with X-linked filamin A (*FLNA*) gene mutations. Chest imaging in these patients characteristically shows severe pulmonary hyperinflation and hyperlucency of multiple lobes of the lungs resembling emphysema along with atelectasis and airway malacia. Extrapulmonary manifestations in patients with *FLNA* gene mutations include periventricular nodular gray matter heterotopia, nystagmus, joint hyperextensibility, congenital heart defects, and vascular aneurysms (Guillerman 2010; Masurel-Paulet et al. 2011; de Wit et al. 2011; Guillerman et al. 2013) (Fig. 5).

3.3 Specific Disorders of Unknown Etiology

3.3.1 Pulmonary Interstitial Glycogenosis

PIG, previously known as infantile cellular interstitial pneumonitis, is characterized histologically by patchy or diffuse infiltration of the interstitium by vimentin-positive immature mesenchymal cells containing abundant cytoplasmic glycogen, without prominent inflammation or fibrosis (Smets et al. 2004). PIG has not been observed beyond infancy, suggesting a relationship of PIG to lung development and growth (Deterding 2010; Deutsch and Young 2010). Patchy PIG is often observed concomitantly with a lung growth abnormality (Deutsch et al. 2007), and may contribute to some exacerbations of CLDI (Dishop 2011) or persistent pulmonary hypertension in infants with congenital heart disease (Radman et al. 2013).

Most patients with PIG present in early infancy with tachypnea and a supplemental oxygen requirement. Pulmonary function testing reveals a restrictive lung disease with marked reduction of pulmonary diffusing capacity. The observations that resolution of PIG on histology and improvement in pulmonary diffusion capacity and forced vital capacity coincide with clinical improvement suggest that PIG impairs respiratory function via alveolar septal thickening (Ehsan et al. 2014), although the ultimate clinical outcome primarily depends upon the severity of any underlying lung growth abnormality (King et al. 2011), and no mortality is associated with cases of isolated PIG. Corticosteroid therapy may hasten the resolution of PIG, possibly due to acceleration of lung maturation rather than to suppression of inflammation (Deterding 2010; Deutsch and Young 2010; Canakis et al. 2002; Onland et al. 2005), but should be used judiciously in this self-limited disorder due to the risks of neuro-developmental impairment, immunosuppression, and poor wound healing associated with corticosteroids (Radman et al. 2013).

Fig. 3 Growth abnormality. A coronal chest CT image from a 15-year-old former preemie with a history of BPD depicts multiple subpleural triangular and linear opacities, and hyperlucent areas resembling emphysema. These findings are commonly observed in adolescent survivors of BPD

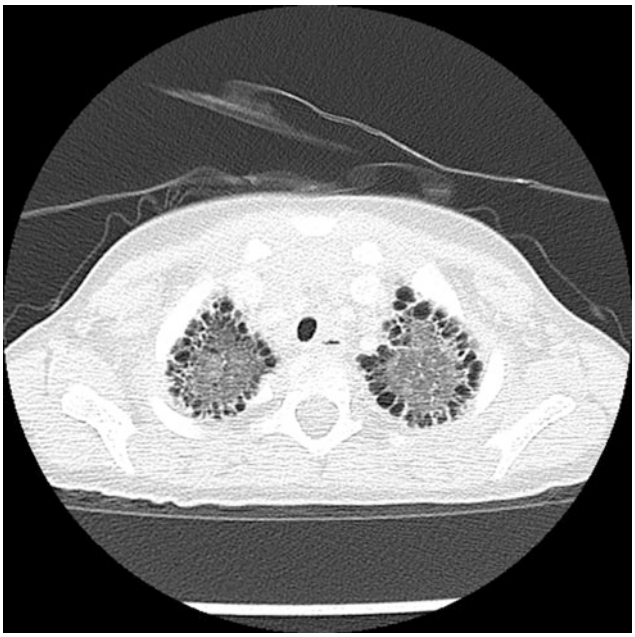

Fig. 4 Growth abnormality. An axial chest CT image from a two-year-old with Down syndrome shows numerous bilateral subpleural cysts. Enlargement of the alveoli and alveolar ducts is particularly marked in the subpleural region in the lung growth abnormality related to Down syndrome

Reported features of PIG on CXR include hyperinflation and interstitial opacities (Smets et al. 2004; Canakis et al. 2002; Onland et al. 2005; Lanfranchi et al. 2010). Reported features of PIG on CT include pulmonary architectural distortion, interstitial thickening, ground-glass opacities, and hyperlucent areas (Smets et al. 2004; Onland et al. 2005; Lanfranchi et al. 2010; Castillo et al. 2010) (Fig. 6). However, these reports describe findings that are at least in part attributable to coexisting lung growth abnormalities. The imaging appearance of PIG in the absence of a concomitant lung growth abnormality is unknown at present, and lung biopsy is currently required for diagnosis.

3.3.2 Neuroendocrine Cell Hyperplasia of Infancy

Neuroendocrine cell hyperplasia of infancy (NEHI), also known as persistent tachypnea of infancy, is characterized histologically by increased numbers of pulmonary neuroendocrine cells (PNECs) and innervated clusters of PNECs called neuroepithelial bodies in the epithelium of the peripheral airways (Deterding et al. 2005). Detection of PNECs on histology is facilitated by special staining for bombesin. PNECs are involved in oxygen sensing and fetal lung development, and rapidly decline in number in normal individuals after the neonatal period. The absence of other significant airway or interstitial disease is an important criterion for the diagnosis of NEHI, since increased numbers of PNECs can also be observed in dissimilar conditions, such as sudden infant death syndrome, BPD, pulmonary hypertension, cystic fibrosis, mechanical ventilation, and smoke exposure (Dishop 2011). NEHI may be associated with minor patchy inflammation or fibrosis in a small proportion of airways (Young et al. 2010). The existence of familial cases of NEHI suggests a genetic etiology for some cases (Popler et al. 2010). Heterozygous mutations in the NK2 homeobox 1 (*NKX*2-1) gene have been reported in a NEHI case, but are not suspected as the predominant cause of NEHI (Young et al. 2013).

NEHI usually presents by six months of age in full-term infants with persistent tachypnea, hypoxemia, and slow weight gain. There is a male predominance. Auscultation may reveal crackles, but wheezing is unusual. The anteroposterior diameter of the chest is often increased. Symptoms can be precipitated or exacerbated by viral respiratory infections or residence at high altitude (Gomes et al. 2013). Lung function tests show peripheral airway obstruction and profound air trapping with reduced forced expiratory flow (FEV) and markedly elevated functional residual capacity (FRC) and residual volume (RV) (Kerby et al. 2013; Lukkarinen et al. 2013). The severity of air trapping as measured by FRC and RV inversely correlates with room air oxygen saturation at short-term (6–12 months) followup, providing a possible prognostic marker. Compared to BPD patients, NEHI patients have similar degrees of airway obstruction, but greater air trapping (Kerby et al. 2013).

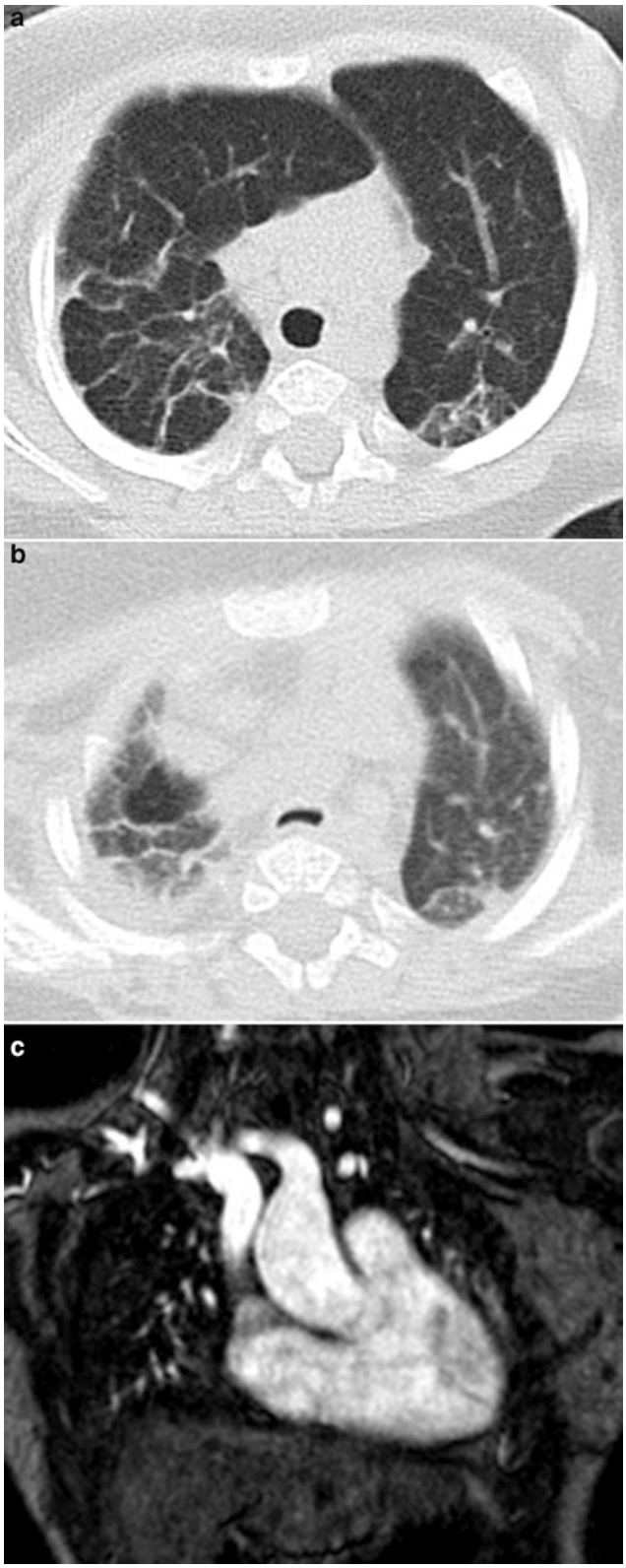

Fig. 5 Growth abnormality. An axial chest CT inspiratory image (**a**) from a six-month-old girl with an X-linked filamin A gene mutation demonstrates severe bilateral pulmonary hyperinflation and scattered atelectasis. The corresponding axial chest CT expiratory image (**b**) reveals narrowing of the trachea related to tracheomalacia. A coronal chest MR angiography image (**c**) obtained at 2 years of age shows dilation of the ascending aorta and innominate artery

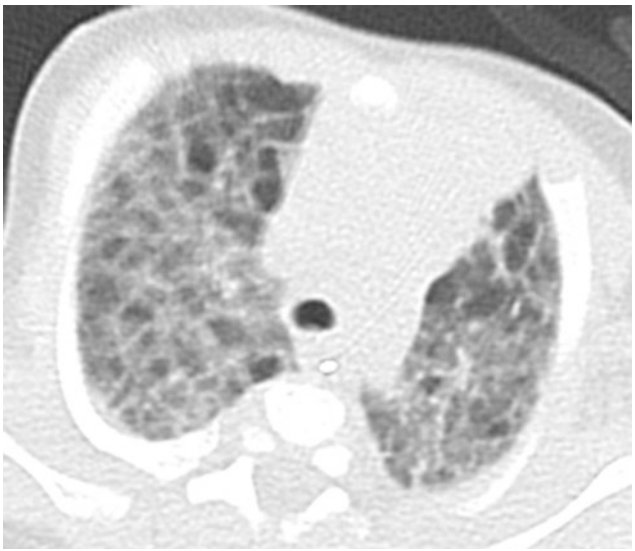

Fig. 6 Pulmonary interstitial glycogenosis. Axial chest CT image from a 7-week-old, former 29-week preemie with hypoxemia shows both ground-glass opacities and hyperlucent pulmonary lobules. Lung biopsy revealed a growth abnormality with superimposed alveolar wall thickening related to pulmonary interstitial glycogenosis

The severity of airway obstruction correlates with the prominence of PNECs (Young et al. 2010). Treatment is largely supportive and focused on oxygen supplementation and nutritional support. Bronchodilators and corticosteroids have not been shown to be beneficial except for treatment of superimposed viral infections (Kerby et al. 2013; Lukkarinen et al. 2013). NEHI is not a life-threatening condition and most patients show clinical and radiographic improvement, especially after two years of age. However, some patients require supplemental oxygen for months to years, and air trapping and exercise intolerance may persist into adolescence (Deterding 2010; Gomes et al. 2013). The development of nonatopic asthma has also been reported in follow-up (Lukkarinen et al. 2013).

On CXR, NEHI manifests with hyperinflation similar to bronchiolitis or reactive airways disease, but without airway wall thickening. CT findings of diffuse air trapping with mosaic attenuation and geographic ground-glass opacities of the right middle lobe, lingula, parahilar, and paramediastinal lung regions are highly characteristic of NEHI, approaching 100 % specificity in the appropriate clinical setting (Fig. 7). Ground-glass opacities may also be present at the peripheral posterior aspects of the lungs. Consolidation, nodules, septal thickening, cysts, and bronchiectasis are usually absent, and the presence of these findings suggests a superimposed or alternative disorder. NEHI is unable to be excluded by CT, since the sensitivity of CT for NEHI is approximately 80 %, and missed diagnosis may occur when the ground-glass opacities are faint or distributed in an atypical pattern (Brody et al. 2010). Due to variability in the number of PNECs, pathologic confirmation of the diagnosis is not

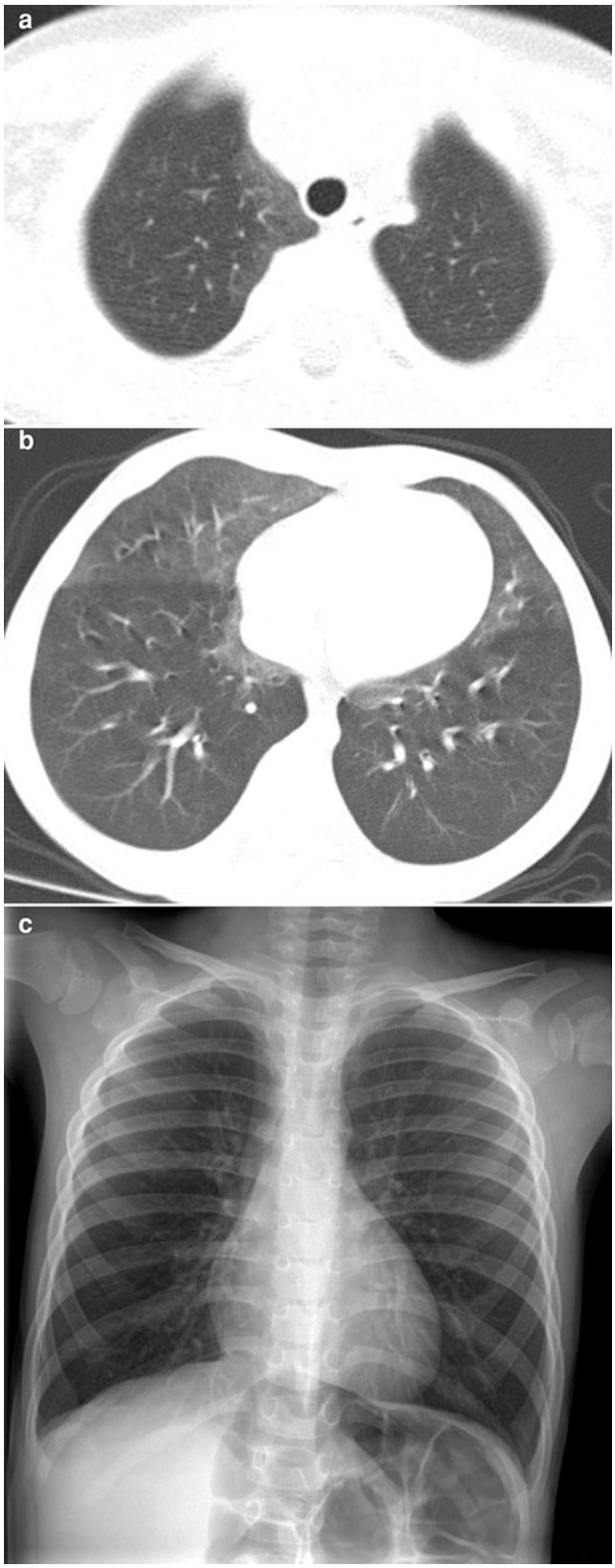

Fig. 7 Neuroendocrine cell hyperplasia of infancy. Axial chest CT images (**a, b**) from a 26-month-old with persistent tachypnea show pulmonary hyperinflation and ground-glass opacities in the right middle lobe, lingula, and paramediastinal regions in a distribution characteristic of neuroendocrine cell hyperplasia of infancy. A frontal CXR (**c**) obtained at 3 years of age shows continued pulmonary hyperinflation

always reliable, especially if airway sampling is limited in the biopsy specimen (Young et al. 2010). A presumptive diagnosis of NEHI can be made without lung biopsy if the clinical presentation and the findings on CT or pulmonary function testing are characteristic (Deterding 2010; Young et al. 2010; Brody et al. 2010; Kerby et al. 2013; Gomes et al. 2013).

3.4 Surfactant Dysfunction Disorders

3.4.1 Genetic Disorders of Surfactant Metabolism

Pulmonary surfactant is composed primarily of phospholipids and surfactant proteins secreted by type II alveolar cells. The lowering of intra-alveolar surface tension by surfactant is required for normal respiratory function. Surfactant also plays a role in innate host defense. Surfactant is cleared by uptake into alveolar epithelial cells or alveolar macrophages under stimulation by granulocyte-macrophage colony-stimulating factor (GM-CSF) (Suzuki et al. 2010).

Genetic disorders of surfactant metabolism are a primary cause of unexplained fatal respiratory distress syndrome (RDS) in term neonates, and are increasingly identified as a cause of chronic DLD in older infants, children, and adolescents. The most frequently identified disease-causing mutations involve the genes encoding ATP binding cassette A3 (ABCA3) (Hamvas 2010) and surfactant protein C (*SP-C*) (Nathan et al. 2012). Other disease-causing mutations may involve the genes encoding surfactant protein B (*SP-B*), colony-stimulating factor 2 receptor alpha (CSFRA), NK2 homeobox 1 (NKX2-1), and solute carrier family 7 amino acid transporter member 7 (SLC7A7) (Nogee 2010).

In young infants presenting with a genetic disorder of surfactant metabolism, histologic findings usually consist of PAP with diffuse alveolar epithelial hyperplasia and foamy macrophages without hyaline membrane formation. With aging, there tends to be a lesser degree of PAP, and histologic findings of lobular remodeling, cholesterol clefts, variable interstitial fibrosis, and interstitial inflammation develop in a CPI or DIP pattern later in infancy or childhood, or in a NSIP pattern later in childhood or adolescence. Endogenous lipoid pneumonia may also be observed. These overlapping histologic patterns limit genotypic-phenotypic correlation, although electron microscopy can be useful for identifying abnormal lamellar bodies that are characteristic of *ABCA3* mutations (Dishop 2010).

The typical clinical presentations and imaging findings of the surfactant dysfunction disorders vary with patient's age. Term neonates unable to produce *SP-B* due to disease-causing biallelic inherited loss-of-function autosomal recessive *SP-B* gene mutations develop severe RDS within hours of birth. CXRs show diffuse hazy granular pulmonary opacification similar to RDS of prematurity (Fig. 8). However, in contrast to RDS of prematurity, infants with genetic

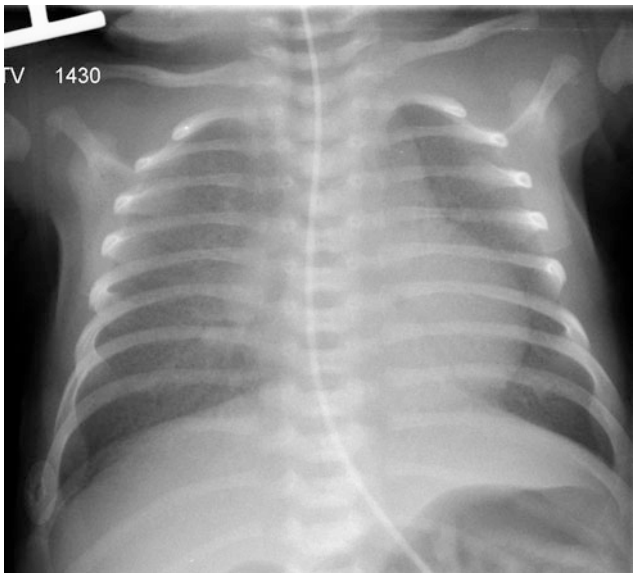

Fig. 8 Surfactant metabolism disorder related to *SP-B* gene mutation. A frontal CXR of a 12-day-old, full-term infant with respiratory distress demonstrates diffuse hazy granular pulmonary opacities resembling the findings usually associated with surfactant deficiency of prematurity

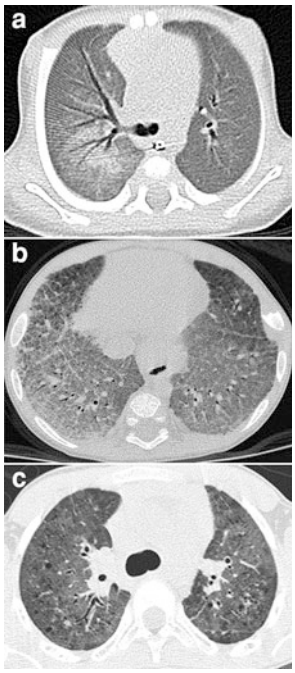

Fig. 9 Surfactant metabolism disorder related to *SP-C* gene mutation. An axial chest CT image (**a**) from a 5-week-old shows diffuse ground-glass opacities and right parahilar consolidation. An axial chest CT image (**b**) from a five-month-old depicts diffuse ground-glass opacities and septal thickening. An axial chest CT image (**c**) from a 9-year-old reveals patchy ground-glass opacities and scattered small parenchymal cysts

SP-B deficiency progress to respiratory failure that is not ameliorated by exogenous surfactant administration. In the absence of lung transplantation, most die within a few months after birth. In rare cases with mutations that allow some *SP-B* production, longer term survival may be feasible (Nogee 2010; Clement et al. 2010).

Variable phenotypes ranging from acute severe RDS in term neonates to chronic DLD in children and adolescents are associated with spontaneous or inherited autosomal dominant *SP-C* gene mutations (Guillot et al. 2009; Thouvenin et al. 2010) or autosomal recessive *ABCA*3 gene mutations (Doan et al. 2008; Flamein et al. 2012). A common clinical presentation of DLD related to *SP-C* or *ABCA*3 gene mutations is cough, tachypnea, and hypoxemia beginning in infancy. Alternatively, affected individuals can remain asymptomatic for years despite progressive fibrosis before sudden life-threatening deterioration occurs. Heterozygosity for an *ABCA*3 mutation can modify the severity of DLD associated with an *SP-C* mutation (Bullard and Nogee 2007). Interestingly, monoallelic *ABCA*3 mutation carriers are overrepresented in infants of >34 weeks gestation age with RDS (Wambach et al. 2012). Treatment with corticosteroids, hydroxychloroquine, or azithromycin may be associated with clinical improvement of patients with genetic disorders of surfactant metabolism, but it is uncertain whether this is entirely due to the therapy or in part to the natural history of the disease, and there are no proven curative therapies except for lung transplantation in the terminal disease phase (Deterding 2010; Nogee 2010; Thouvenin et al. 2010).

CXRs of young infants with disease-causing *SP-C* or *ABCA*3 gene mutations demonstrate diffuse or patchy hazy granular pulmonary opacities, while CT scans show diffuse ground-glass opacities, consolidation, septal thickening, or crazy-paving (Doan et al. 2008; Olsen et al. 2004; Stevens et al. 2005; Prestridge et al. 2006; Soraisham et al. 2006). In older infants and children, the ground-glass opacities tend to decrease and thin-walled cysts develop and increase in number and size with age (Doan et al. 2008; Mechri et al. 2010; Flamein et al. 2012) (Fig. 9). Possibly as an effect of chronic restrictive lung disease on the growing chest wall, pectus excavatum often develops in patients with DLD related to *ABCA*3 mutations who survive infancy (Doan et al. 2008). Changes in lung findings on CT do not correlate with lung function or outcome in patients with DLD related to *ABCA*3 mutations, and there is no established role for routine chest imaging after the diagnosis has been established (Doan et al. 2008).

Understanding of the spectrum of genetic disorders associated with surfactant dysfunction and pediatric DLD continues to broaden. NK2 homeobox 1 (NKX2-1), also known as thyroid transcription factor-1 (TTF-1), is expressed in the forebrain, thyroid, and lung, and regulates transcription of the genes for surfactant proteins and Clara cell secretory protein. Disease-causing sporadic or inherited autosomal dominant *NKX*2-1 gene mutations or deletions

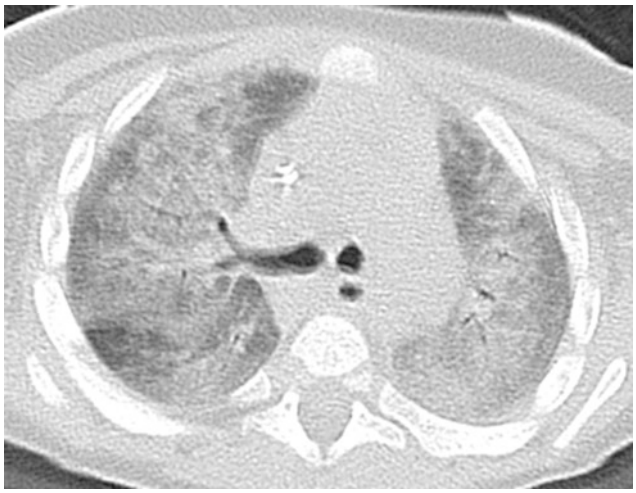

Fig. 10 Surfactant metabolism disorder related to *NKX*2-1 gene mutation. Bilateral patchy ground-glass opacities are shown on an axial chest CT image from a 13-month-old with chorea, hypotonia, hypothyroidism, and chronic pneumonitis of infancy as manifestations of the "brain-lung-thyroid" syndrome

can lead to maldevelopment of the basal ganglia and thyroid and decreased production of surfactant proteins, resulting in "brain-lung-thyroid syndrome" characterized by congenital hypothyroidism, hypotonia, chorea, and lung disease. Only a slight majority of cases manifest with the full syndrome, and there is isolated lung disease in one-fifth of cases at presentation. Mortality related to the lung disease is around 20 % (Carre et al. 2009; Hamvas et al. 2013). Clinical manifestations of the lung disease are varied and illustrate the diverse role NKX2-1 plays in surfactant function, alveolarization, and innate immunity. The presenting pulmonary phenotype is severe neonatal RDS in about three-fourths of cases and chronic childhood DLD in about one-fifth of cases. Recurrent respiratory infections are also common (Guillot et al. 2010; Hamvas et al. 2013). The histology is heterogeneous, and may include changes of PAP, CPI, DIP, NSIP, or growth abnormality with alveolar simplification. CT findings include diffuse or patchy ground-glass opacities, consolidations, and cysts (Galambos et al. 2010; Hamvas et al. 2013) (Fig. 10). Thyroid ultrasonography or scintigraphy reveals thyroid hypoplasia, hemiagenesis or athyreosis in 45 % of cases (Carre et al. 2009). Intriguingly, a case of NEHI associated with *NKX*2-1 mutations has been reported, suggesting that NEHI may result from altered expression of genes regulated by NKX2-1 other than those in the surfactant system (Young et al. 2013).

Homozygous or compound heterozygous mutations or deletions of the gene encoding colony-stimulating factor 2 receptor alpha (CSF2RA), also known as granulocyte-macrophage colony-stimulating factor receptor alpha (GM-CSFRA), can severely reduce GM-CSF receptor signaling and impair alveolar macrophage function. This results in PAP that is characterized by filling of alveoli with surfactant and foamy macrophages and preservation of normal alveolar walls, in contrast to the disorders of surfactant production associated with *SP-B*, *SP-C,* or *ABCA*3 mutations, in which alveolar epithelial hyperplasia and lobular remodeling occur. Children with heredity PAP related to *CSF*2*RA* gene mutations or deletions develop progressive dyspnea, exercise intolerance, or tachypnea at 1–9 years of age, with a mean age of 5 years at symptom onset. The clinical course is often insidious and initial misdiagnosis as asthma or pneumonia is common. Serum and bronchoalveolar (BAL) fluid characteristically show elevated GM-CSF levels. The PAP is typically patchy, leading to patchy pulmonary airspace opacities on CXR and geographic ground opacities and crazy-paving on chest CT (Suzuki et al. 2008; Martinez-Moczygemba et al. 2008; Suzuki et al. 2010). Whole-lung lavage therapy results in clinical and radiographic improvement (Fig. 11), in contrast to patients with disorders of surfactant production who do not respond well to lavage therapy (Suzuki et al. 2010).

Lysinuric protein intolerance (LPI) is a multisystem disease resulting from an inherited defect of cationic amino acid transport attributable to autosomal recessive *SLC7A7* gene mutations. LPI is associated with dietary protein intolerance, failure to thrive, osteoporosis, hepatosplenomegaly, hemophagocytic lymphohistiocytosis, immune dysfunction, nephropathy, and lung involvement (Ogier de Baulny et al. 2012). The lung involvement can occur at any age, including childhood, and is characterized by endogenous lipoid pneumonia, PAP, or pulmonary hemorrhage. CT is a sensitive test for diagnosing early lung involvement that manifests as septal thickening, nodules, and subpleural cysts prior to the onset of respiratory symptoms or pulmonary function test abnormalities (Santamaria et al. 1996). Some patients rapidly progress to respiratory failure with widespread pulmonary airspace opacities on CXR and CT related to PAP from alveolar macrophage dysfunction (Parto et al. 1993; Ogier de Baulny et al. 2012). LPI is generally treated with dietary protein restriction and L-citrulline supplementation. The lung involvement can be treated with corticosteroids and whole-lung lavage (Ogier de Baulny et al. 2012).

Recognition of clinical and radiographic findings suggestive of a surfactant dysfunction disorder is important, since the diagnosis may then be confirmed by genetic testing for surfactant gene mutations, avoiding the risk of lung biopsy. Lung biopsy may still be appropriate if genetic testing is nondiagnostic or if awaiting genetic testing results would delay the diagnosis in patients with rapidly progressive disease requiring lung transplantation for continued survival (Doan et al. 2008; Mechri et al. 2010). Occasionally, cases are encountered with imaging and histologic findings suggestive of a surfactant dysfunction disorder, but genetic testing for known disease-causing mutations is negative. Some of these

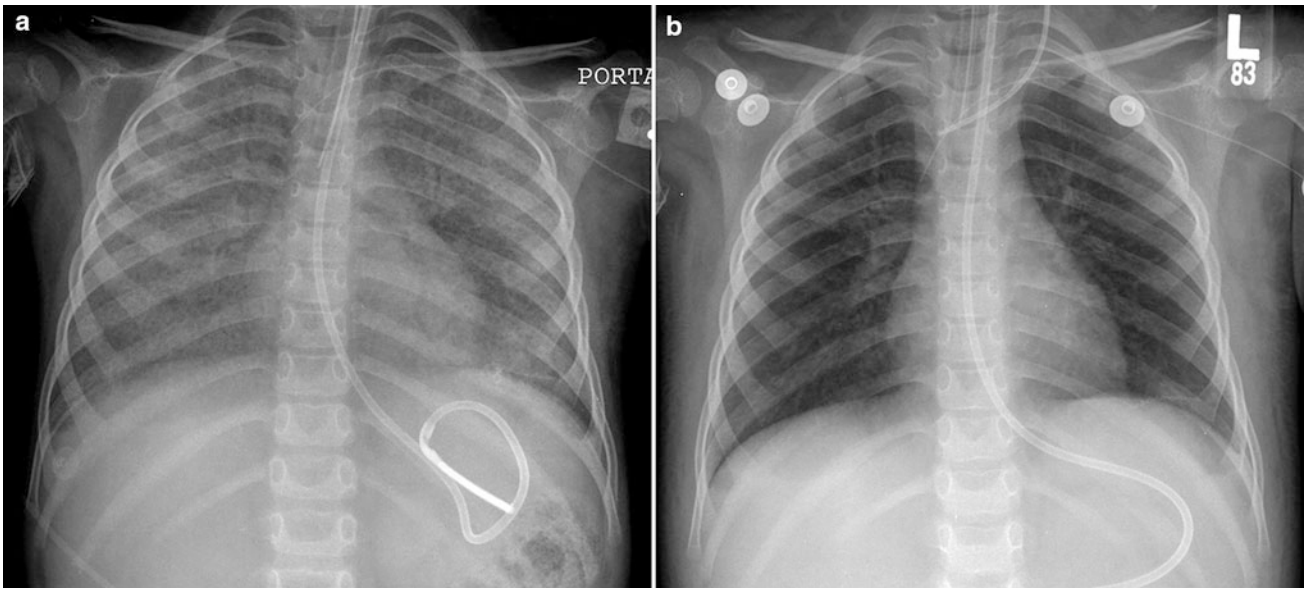

Fig. 11 Surfactant metabolism disorder related to *CSF2RA* mutation. A frontal CXR (**a**) of a 3-year-old demonstrates diffuse pulmonary airspace opacification. Disrupted GM-CSF receptor signaling in this genetic disorder results in impaired alveolar macrophage function and pulmonary alveolar proteinosis. Dramatic improvement in lung aeration is shown on a frontal CXR (**b**) following whole-lung lavage

cases are likely related to as yet characterized genetic defects of surfactant metabolism, especially in those with a family history of unexplained childhood-onset DLD.

3.4.2 Autoimmune Pulmonary Alveolar Proteinosis

Pediatric PAP is not always attributable to genetic disorders of surfactant metabolism. The catabolism of surfactant by alveolar macrophages can be impaired in multiple acquired conditions, including autoimmune disorders, leukemia, and toxic exposures (Dishop 2010). Autoimmune PAP due to neutralizing autoantibodies to GM-CSF that interfere with alveolar macrophage signaling is the most common cause of sporadic PAP in adults and may present in childhood or adolescence. As with hereditary PAP related to *CSF2RA* genetic defects, the CT findings include ground-glass opacities, septal thickening, and crazy-paving (Fig. 12). CT can be used to monitor the response of autoimmune PAP to therapy with whole-lung lavage and aerosolized GM-CSF (Robinson et al. 2009).

3.5 Disorders Related to Systemic Disease Processes

A large, diverse group of systemic disease processes is associated with pediatric DLD. These include vasculitis, connective tissue diseases, granulomatous disorders, lymphoid hyperplasia and lymphoproliferative disorders, primary and secondary immunodeficiencies, lysosomal storage disorders, and Langerhans cell histiocytosis. The clinical presentations and imaging appearances of these disease processes are covered in the chapter entitled Thoracic Manifestations of Systemic Diseases by Holland, Guillerman, and Brody in this book.

3.6 Disorders of the Normal Immunocompetent Host

3.6.1 Bronchiolitis Obliterans

The clinical syndrome of bronchiolitis obliterans (BO) is characterized histologically by constriction or obliteration of the lumens of small airways by a fibroblastic reparative response to injury. The inciting event is typically a respiratory infection (especially adenovirus, influenza virus, or *Mycoplasma pneumoniae*) with extensive airway mucosal necrosis. Other preceding conditions include Stevens-Johnson syndrome, toxic inhalational injury, graft-versus-host disease, and chronic airway rejection in the setting of lung transplantation (Dishop 2010). There is a predominance of male patients. The time interval between infection and symptoms and signs of obstructive lung disease, such as wheezing, tachypnea, and dyspnea is variable and can be as short as a few months, although the diagnosis after onset of symptoms is often delayed for many months (Lino et al. 2013).

CXRs in patients with BO often show hyperinflation, but CXRs are generally nonspecific and insensitive. Characteristic findings of post-infectious pediatric BO on CT include increased lung volume, bronchiectasis, bronchial

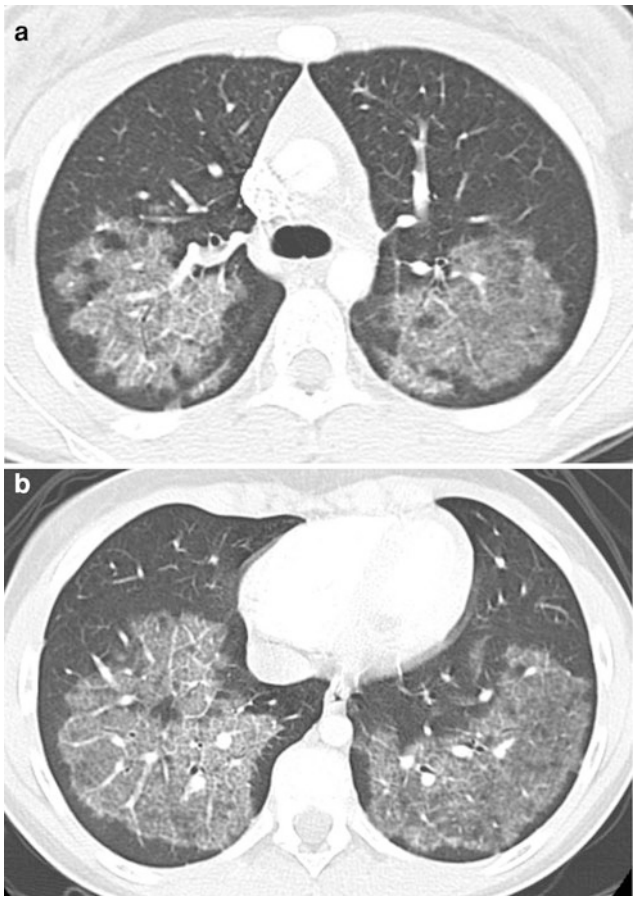

Fig. 12 Surfactant metabolism disorder related to autoantibodies to GM-CSF. Axial chest CT images (**a, b**) from an 11-year-old show geographic ground-glass opacities and crazy-paving. Autoantibodies to GM-CSF in this autoimmune disorder result in impaired alveolar macrophage function and pulmonary alveolar proteinosis

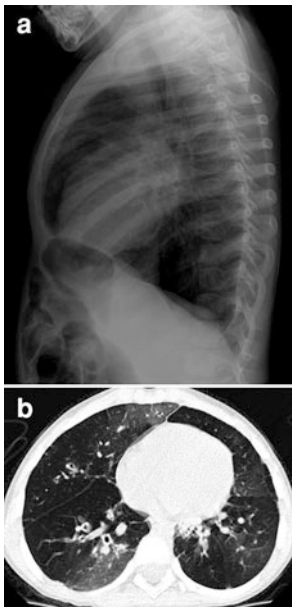

Fig. 13 Bronchiolitis obliterans. A lateral CXR (**a**) of a 4-year-old with a history of influenza, respiratory syncitial virus, and *Mycoplasma* pneumonia shows marked pulmonary hyperinflation with diaphragmatic flattening and widening of the retrosternal clear space. A corresponding axial chest CT image (**b**) reveals bronchiectasis, bronchial wall thickening, mosaic attenuation, and pulmonary vascular attenuation in hyperlucent regions

wall thickening, mosaic attenuation, parenchymal hyperlucency, pulmonary vascular attenuation, and expiratory air trapping (Yalcin et al. 2003; Zhang et al. 1999; Bandeira et al. 2011; Lino et al. 2013) (Fig. 13). Hyperlucency, mosaic attenuation, air trapping, and bronchiectasis tend to be more marked in BO than in problematic severe asthma (Bandeira et al. 2011). The combination of a typical clinical history, adenovirus infection, and mosaic attenuation on CT is highly specific for post-infectious BO in young children (Colom and Teper 2009). CT offers the ability to survey the entire lungs, while the heterogeneous distribution of airway involvement in BO poses the risk of a false-negative biopsy from inadequate tissue sampling (Moonnumakal and Fan 2008). A confident diagnosis of BO can be made without the need for lung biopsy in the setting of a child with a suggestive clinical presentation, a fixed obstructive pattern on pulmonary function testing, and characteristic CT findings. The combination of pulmonary vascular attenuation and hyperlucency on CT is highly specific for moderate or severe nontransplant BO in children (Smith et al. 2011). However, the sensitivity of CT for moderate or severe nontransplant BO in children is only modest, so that CT cannot exclude BO (Smith et al. 2011). CT is valuable as a prognostic tool since severe abnormalities on CT in children under three years of age with post-infectious BO predict poor lung function several years later (Mattiello et al. 2010).

Swyer-James-MacLeod syndrome is a variant of BO that typically presents with a hyperlucent hypovascular lung of small or normal volume on CXR several months or a few years after the inciting infection. In about a half of cases of Swyer-James-MacLeod syndrome, the findings of BO are actually found to be bilateral if CT is performed (Lucaya et al. 1998).

3.6.2 Eosinophilic Pneumonia

The eosinophilic lung diseases are a diverse group of disorders that are often, but not always, associated with peripheral eosinophilia. These disorders can be acute or chronic, idiopathic or secondary to parasitic infections or drug reactions, and isolated to the lungs or involve extrapulmonary tissues. In addition to suggesting the diagnosis of an eosinophilic lung disease, imaging can be useful in assessing the response to therapy (Oermann et al. 2000). The thoracic imaging findings vary with the type of disorder.

Simple eosinophilic pneumonia is often related to drug reaction or parasitic infection, but can be idiopathic. Affected patients can have cough, fever, dyspnea, and hypoxia, although some are asymptomatic. Imaging demonstrates patchy pulmonary ground-glass opacities or consolidations that are often migratory and peripheral (Fig. 14). Clinical and radiographic improvement usually occurs

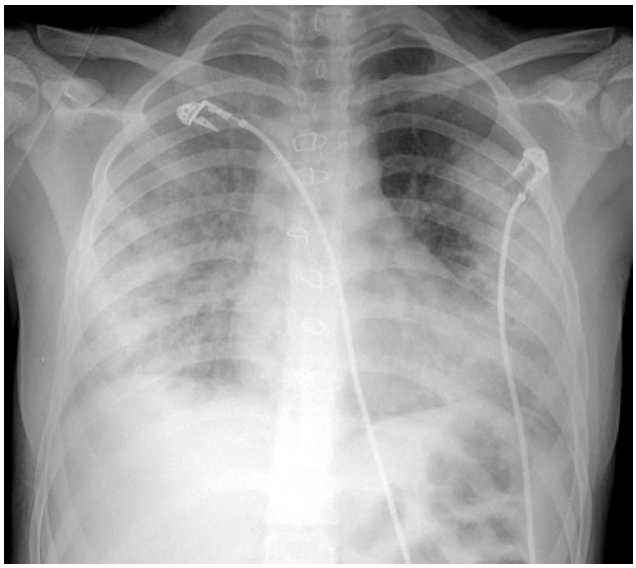

Fig. 14 Drug-induced eosinophilic pneumonia. A frontal CXR of a 17-year-old with acute hypoxemia and a history of lung transplantation for cystic fibrosis shows extensive bilateral pulmonary airspace opacities that are most pronounced peripherally. BAL lavage demonstrated increased eosinophils. The pneumonia resolved after discontinuation of the inciting drug, doxycycline

Fig. 15 Bronchocentric granulomatosis. An axial chest CT image from a 2-year-old depicts multiple, airway-centric, nodular, and short tubular opacities in the right lung related to granulomatous lesions along the airways with endoluminal plugging

promptly after discontinuation of the inciting drug, although corticosteroids may be administered in severe or persistent cases.

The findings of airspace opacities, septal thickening, and pleural effusions typical of idiopathic acute eosinophilic pneumonia (AEP) can be misconstrued as pulmonary edema. A presumptive diagnosis of AEP can be made without biopsy in children with these imaging findings, fever, acute respiratory failure requiring ventilatory support, and marked eosinophilia on BAL (Vece and Fan 2011). Some cases of AEP are thought to be precipitated by exposure to irritants such as smoke. Treatment with corticosteroids usually results in rapid clinical improvement and resolution of radiographic abnormalities.

Idiopathic chronic eosinophilic pneumonia (CEP) is characterized by peripherally-predominant consolidation or ground-glass opacities, marked eosinophilia in BAL fluid or peripheral blood, respiratory symptoms for greater than 4 weeks, and absence of other known causes of eosinophilic lung disease. The diagnosis can also be made with consistent lung biopsy findings in cases without clinical and radiographic improvement after first-line corticosteroid treatment. Many cases of idiopathic CEP are initially misdiagnosed as asthma, and a subset of persistent cases develop reticulonodular interstitial opacities and cysts (Giovannini-Chami et al. 2014).

Idiopathic hypereosinophilic syndrome (IHES) predominantly affects males and is characterized by prolonged eosinophilia and multiorgan damage (especially of the lungs, skin, heart, and nervous system) due to eosinophilic infiltration. Nodules with ground-glass halos are seen in IHES. Allergic bronchopulmonary aspergillosis (ABPA) is characterized by asthma and noninvasive colonization of dilated airways by *Aspergillus*. There may also be patchy peribronchial eosinophilic pneumonia. Imaging shows central bronchiectasis with or without mucoid impaction. Bronchocentric granulomatosis (BCG) develops as an abnormal cell-mediated response to *Aspergillus* and may be part of the spectrum of ABPA or occur as an isolated disorder. BCG is characterized by destructive granulomatous lesions along the bronchi and bronchioles with intraluminal inspissations and surrounding eosinophilic pneumonia, resulting in airway-centric nodular, "sausage-like," or consolidative opacities on imaging (Jeong et al. 2007; Kradin and Mark 2008) (Fig. 15). Eosinophilic granulomatosis with polyangiitis (EGPA), formerly known as Churg-Strauss syndrome, is a life-threatening systemic necrotizing vasculitis that commonly involves the lungs, upper airway, musculoskeletal system, gastrointestinal system, nervous system, skin, and heart. Subpleural consolidation, centrilobular nodules, bronchial wall thickening, and septal thickening are typical pulmonary imaging manifestations of EGPA (Gendelman et al. 2013).

3.6.3 Hypersensitivity Pneumonitis

Hypersensitivity pneumonitis is characterized on histology by lymphocytic infiltration of the bronchioles and adjacent interstitium, with giant cells and poorly formed non-necrotizing granulomas distributed around the bronchioles.

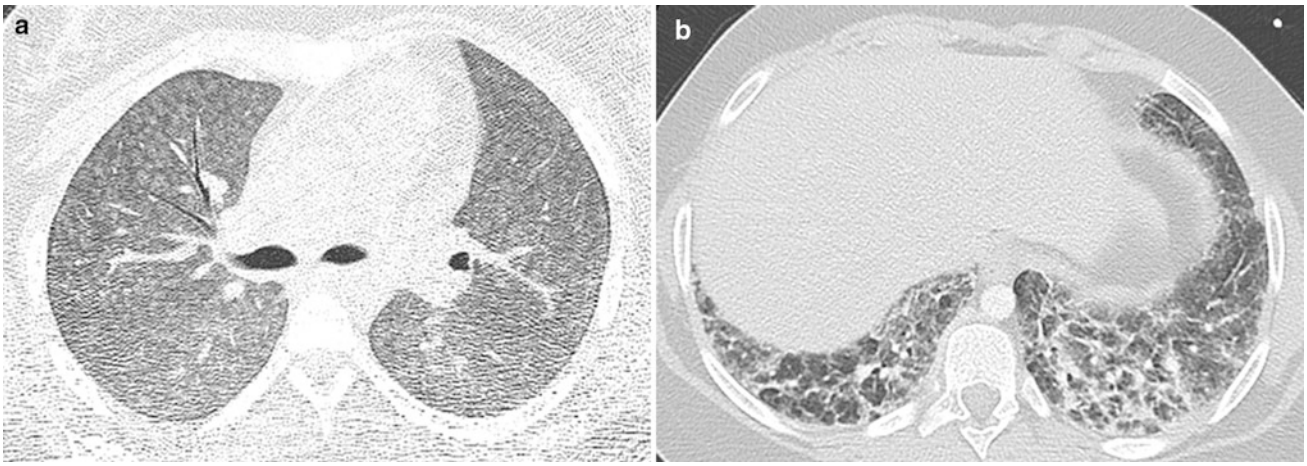

Fig. 16 Hypersensitivity pneumonitis. An axial chest CT image (**a**) from a 14-year-old with cough and repetitive bird exposure reveals diffuse centrilobular nodular ground-glass opacities typical of the subacute phase. An axial chest CT image (**b**) from a 10-year-old with fatigue and repetitive bird exposure shows coarse reticular opacities and architectural distortion at the lung bases compatible with fibrosis in the chronic phase

A NSIP pattern with interstitial fibrosis and cystic remodeling may be observed in the chronic setting (Dishop 2010). Birds, pets, and molds are the most common precipitating agents in children. Other causes include highly reactive low-molecular-weight compounds in spray paints, epoxy resins, glues, and insecticides, as well as drugs such as methotrexate (Vece and Fan 2010). There is a mean lag time of 11 months from symptom onset to diagnosis, and a meticulous environmental exposure history is a crucial step in the clinical evaluation. The most common symptom is dyspnea with exercise, followed by dyspnea at rest, dry cough, and weight loss. CXRs are limited in sensitivity, being normal in over one-third of cases at initial presentation (Buchvald et al. 2011). The absence of serum-precipitating antibodies does not exclude the diagnosis (Clement et al. 2010; Vece and Fan 2010). A presumptive diagnosis without biopsy can be made in children with an exposure history and positive precipitins, lymphocytosis on BAL, and typical findings on CT (Vece and Fan 2011). Consolidation and ground-glass opacities that can mimic infection or edema are typical on CT in the acute phase. Ill-defined centrilobular nodules, ground-glass opacities, and low attenuation foci of air trapping are characteristic of the subacute phase. Irregular linear or reticular opacities, architectural distortion, and honeycombing indicative of fibrosis can be observed in the chronic phase (Fig. 16). If there is ongoing exposure to the inciting antigen, there can be findings of multiple phases superimposed. The imaging findings associated with the acute and subacute phases usually regress after treatment with corticosteroids and elimination of exposure to the offending antigen, but fibrosis from the chronic phase may persist (Hartman 2003; MacDonald and Müller 2003; Buchvald et al. 2011).

3.6.4 Aspiration Pneumonia

While most common in the setting of profound neuromuscular or developmental disorders, silent aspiration can also occur in otherwise healthy children. If unrecognized and untreated, recurrent aspiration can lead to unexplained DLD. The associated clinical signs and symptoms of cough, tachypnea, and fever are nonspecific. The presence of increased lipid-laden macrophages on BAL or lung biopsy is also not specific for aspiration, as this can be observed with other conditions, such as resolving hemorrhage, pneumonia, and surfactant disorders. CT can play an important role in suggesting the correct diagnosis. The findings of bronchiectasis and tree-in-bud centrilobular opacities, especially in dependent lung regions, are suggestive of aspiration. Exogenous lipoid pneumonia, most frequently noted in children administered mineral oil for chronic constipation, manifests with consolidation, ground-glass opacities, and crazy-paving on CT (Fig. 17). The finding of fatty attenuation in the lungs as a sign of lipoid pneumonia on CT is of limited value since it may be either obscured or simulated by volume averaging of nonfatty inflammatory exudate and air (Zanetti et al. 2007; Marchiori et al. 2010).

3.6.5 Acute Interstitial Pneumonia

Diffuse alveolar damage (DAD) is a histopathologic pattern with an exudative phase characterized by edema, hyaline membranes, and interstitial acute inflammation, and an organizing phase characterized by loose organizing fibrosis, alveolar wall thickening, type II pneumocyte hyperplasia, and alveolar collapse. The term diffuse in DAD refers to involvement of all constituents of the alveolar wall, and there are often patchy areas of spared lung (Kligerman et al. 2013). DAD is a nonspecific reaction to variety of insults and can be

Fig. 17 Aspiration pneumonia. Axial chest CT image from a 17-year-old shows widespread crazy-paving from exogenous lipoid pneumonia related to repetitive aspiration of mineral oil administered for constipation

associated with acute respiratory distress syndrome (ARDS), infection (especially CMV or *Pneumocystis*), toxic inhalation, drug reaction, bone marrow transplantation, primary graft dysfunction in lung transplant recipients, and idiopathic acute interstitial pneumonia (AIP).

AIP has a rapidly progressive course leading to respiratory failure, and can occur in previously healthy children (Liu et al. 2011). The typical CT findings of AIP are patchy or geographic ground-glass opacities and dependent consolidation, followed by architectural distortion and traction bronchiectasis (Bouros et al. 2000). The differential diagnosis includes infectious pneumonia, pulmonary edema, pulmonary hemorrhage, PAP, and AEP (Fan et al. 2004). Although the abnormal pulmonary findings on imaging can resolve, many patients are left with residual fibrosis that is most pronounced in the nondependent portions of the lung (Fig. 18), possibly related to protection of the collapsed dependent lung from oxygen toxicity and barotrauma incurred during treatment (Kligerman et al. 2013).

3.6.6 Cryptogenic Organizing Pneumonia

Organizing pneumonia is characterized histologically by fibroblastic tissue in the distal bronchioles, alveolar ducts, and alveoli. Organizing pneumonia in children can be idiopathic or secondary to processes that incite a reparative response in the lung, such as infection, aspiration pneumonia, autoimmune disease, asthma, drug reaction, chemotherapy, and bone marrow transplantation (Fan et al. 2004). When idiopathic, it is termed cryptogenic organizing pneumonia (COP). The typical clinical presentation of COP is a subacute illness with nonproductive cough and dyspnea. The appearance of COP on CT is highly variable, with the most frequent pattern consisting of peripheral or peribronchovascular patchy consolidation with or without surrounding ground-glass opacities. Air bronchograms and mild bronchial dilation are common within the sites of consolidation, which can be migratory. Other patterns include the "atoll" or "reverse halo" sign (central ground-glass opacity surrounded by a ring of consolidation), perilobular thickening, and arciform or band-shaped subpleural opacities (Polverosi et al. 2006) (Fig. 19). A majority of cases of COP recover completely with corticosteroid treatment, but some cases may relapse or undergo progressive fibrosis resulting in reticular opacities and traction bronchiectasis resembling NSIP (Travis et al. 2013; Kligerman et al. 2013).

3.6.7 Idiopathic Nonspecific Interstitial Pneumonia

Despite the misleading name, NSIP is a distinct clinical entity characterized histologically by spatially and temporally uniform interstitial thickening with a varying spectrum of cellular to fibrosing patterns (Travis et al. 2008). In children, it can be idiopathic or associated with autoimmune connective tissue disorders, familial pulmonary fibrosis, genetic disorders of surfactant metabolism, or chronic hypersensitivity pneumonitis. The most common symptoms are dyspnea and cough. The most frequently observed findings on CT are peripheral or diffuse ground-glass and fine linear or reticular opacities predominantly involving the lower lung zones. Cysts, traction bronchiectasis, volume loss, and honeycombing may develop over time (Fig. 20). NSIP can resolve, remain stable, or progress (Kligerman et al. 2009).

3.6.8 Idiopathic Pulmonary Hemosiderosis

Idiopathic pulmonary hemosiderosis (IPH) is characterized by BAL showing abundant hemosiderin-laden macrophages and lung biopsy showing "bland" pulmonary hemorrhage without vasculitis. The median age at diagnosis is 4 years and the most common clinical manifestations are dyspnea and anemia. Hemoptysis occurs in no more than half of cases, and delay in diagnosis is common (Taytard et al. 2013). Other disorders capable of causing pulmonary hemorrhage, such as respiratory tract infections, airway neoplasms, bronchiectasis, coagulopathies, pulmonary venous hypertension, and pulmonary arteriovenous malformations, should be excluded before a diagnosis of IPH is made. IPH is associated with cow's milk allergy (Heiner syndrome) (Moissidis et al. 2005), celiac disease (Lane-Hamilton syndrome) (Hendrickx et al. 2011), and Down syndrome (Taytard et al. 2013). Imaging findings can include airspace opacities, nodules, septal thickening, cysts, and honeycombing (Fig. 21). CT is useful for monitoring the response to therapy with corticosteroids or other immunosuppressants. Lung biopsy is advocated for children with anemia and pulmonary opacities, hemoptysis, or hemosiderin-laden macrophages on BAL, even in the absence of anti-neutrophil cytoplasmic antibodies (ANCA),

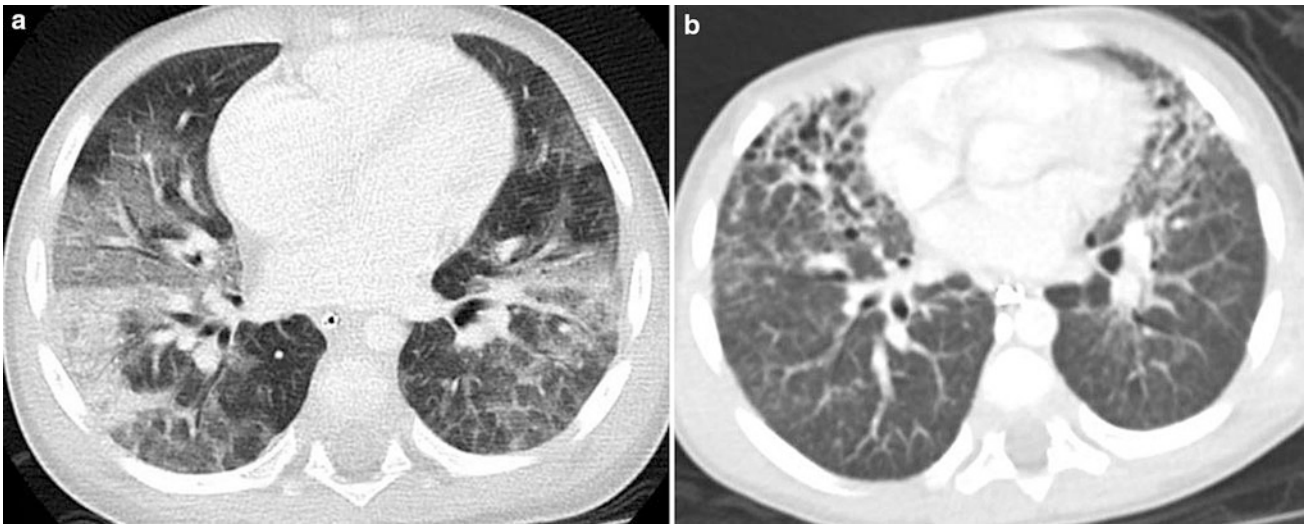

Fig. 18 Acute interstitial pneumonia. An axial chest CT image (**a**) from a 2-year-old with fever and acute respiratory failure shows patchy bilateral ground-glass opacities and consolidation related to diffuse alveolar damage. An axial chest CT image (**b**) obtained 3 weeks later reveals traction bronchiectasis and architectural distortion of the anterior nondependent lung regions related to fibrosis

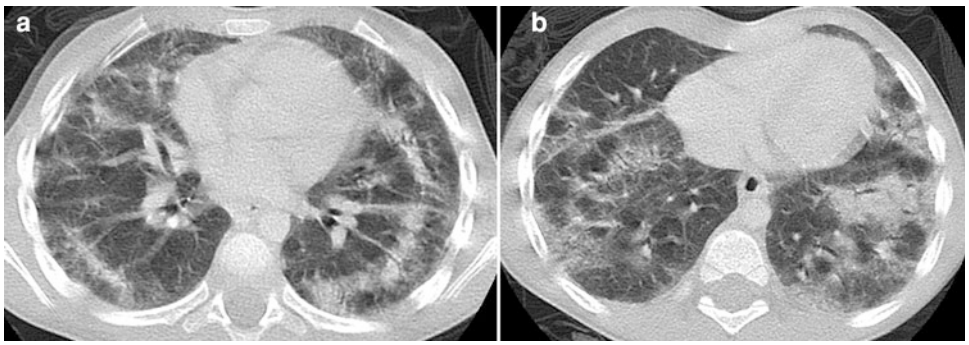

Fig. 19 Cryptogenic organizing pneumonia. Axial chest CT images (**a, b**) from a 3-year-old with hypoxemia depicts peripheral arciform and patchy peribronchial foci of consolidation

since many of these patients will have capillaritis that confers a worse prognosis than IPH (Vece and Fan 2011). Pulmonary capillaritis is further discussed in the chapter entitled Thoracic Manifestations of Systemic Diseases by Holland, Guillerman, and Brody in this book.

3.7 Vascular Disorders Masquerading as Diffuse Lung Disease

The chILD Research Cooperative classification (Deutsch et al. 2007) and expanded chILD classification (Rice et al. 2013) acknowledge the presence of certain vascular disorders with clinical and imaging features that can mimic childhood DLD. These includes disorders such as congestive heart failure, cor triatriatum, congenital mitral stenosis, anomalous pulmonary venous return, pulmonary vein stenosis, pulmonary vein atresia, and pulmonary veno-occlusive disease (PVOD) that are associated with transudative pulmonary edema from pulmonary venous congestion or obstruction. Also included are disorders such as lymphangiectasia and lymphangiomatosis that are associated with impaired clearance of interstitial lung fluid.

3.7.1 Pulmonary Veno-Occlusive Disease

PVOD is characterized by fibrous obstruction of the post-capillary pulmonary septal veins and pre-septal venules, resulting in pulmonary hypertension, transudative pulmonary edema, and capillary proliferation. PVOD can be idiopathic or associated with connective tissue disease, HIV infection, organ transplantation, chemotherapy, or toxic exposures. Patients with PVOD often present with progressive dyspnea with exertion, and delay in diagnosis is common (Woerner et al. 2014). Typical features of PVOD include normal pulmonary capillary wedge pressure, low pulmonary diffusing capacity, hypoxemia at rest, desaturation with exercise, and occult alveolar hemorrhage on BAL.

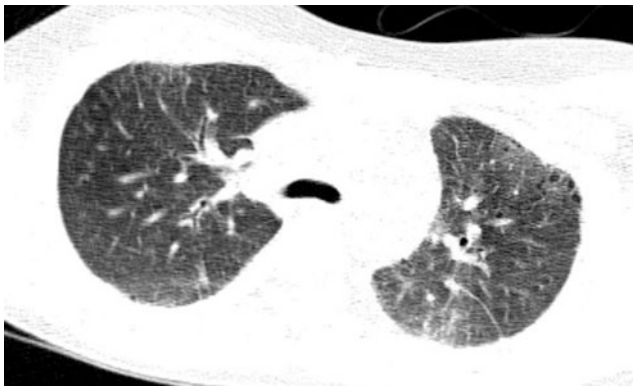

Fig. 20 Nonspecific interstitial pneumonia. An axial CT image from a 13-year-old with cough and a family history of pulmonary fibrosis demonstrates peripheral fine, linear, and ground-glass opacities bilaterally along with scattered tiny cysts and volume loss of the left lung

Characteristic findings of PVOD on CT include smooth septal thickening, lobular ground-glass opacities, pleural effusions, enlargement of mediastinal and hilar lymph nodes, enlargement of the central pulmonary arteries and right heart chambers, and normal appearance of the main pulmonary veins and left heart chambers (Frazier et al. 2007; Montani et al. 2009; Woerner et al. 2014) (Fig. 22). PVOD accounts for 5–10 % of cases initially suspected as idiopathic pulmonary arterial hypertension (PAH) (Montani et al. 2009). It is crucial not to misdiagnose PVOD as idiopathic PAH since the vasodilators used to treat PAH patients can induce fulminant pulmonary edema in patients with PVOD. Pulmonary artery enlargement and mosaic lung attenuation can be seen in either PVOD or PAH, but septal thickening, lobular ground-glass opacities, lymphadenopathy, and pleural effusions are typical of PVOD, but not PAH (Frazier et al. 2007). A presumptive diagnosis of PVOD can be made on the basis of characteristic findings of CT, arterial blood gases, pulmonary function testing, and BAL, thereby avoiding high-risk lung biopsy in these patients. Early recognition is crucial, since PVOD has a poor prognosis with a mean reported survival time of only 14 months after diagnosis, and lung transplantation is the only curative therapy (Montani et al. 2009; Woerner et al. 2014).

3.7.2 Pulmonary Lymphangiectasia

Pulmonary lymphangiectasia is characterized histologically by dilation of the lymphatics draining the interstitial and subpleural spaces. Pulmonary lymphangiectasia can be a primary disorder or occur secondary to lymphatic congestion from conditions associated with excessive lung fluid accumulation such as congestive heart failure or obstructed pulmonary veins. Pulmonary lymphangiectasia can also be present as part of the histologic findings in alveolar capillary dysplasia with misalignment of the pulmonary veins

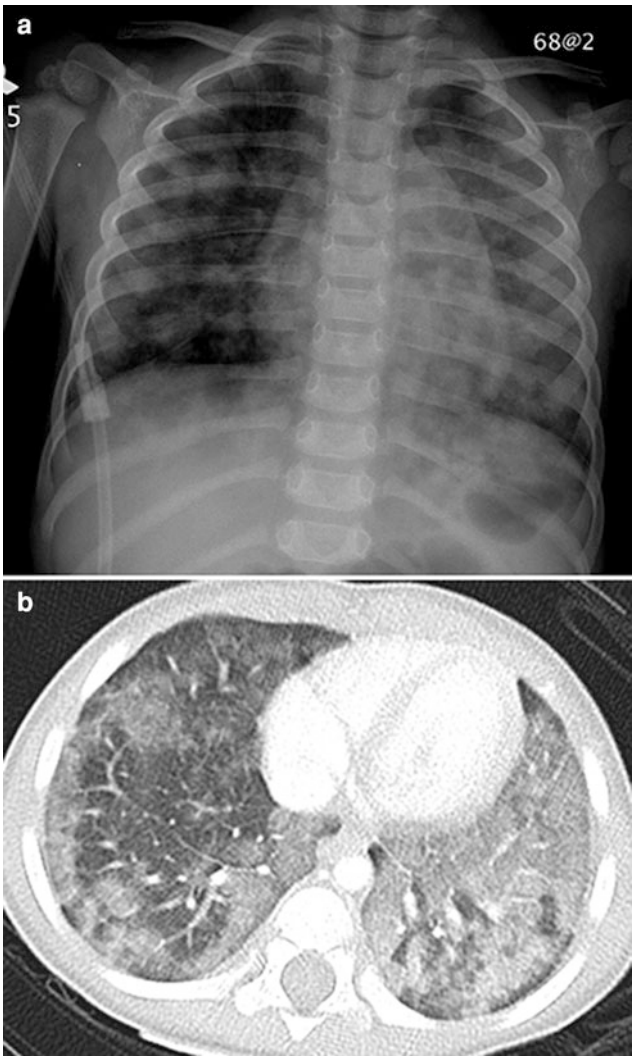

Fig. 21 Idiopathic pulmonary hemosiderosis. A frontal CXR (**a**) of a 1-year-old with anemia and a corresponding axial chest CT image (**b**) show patchy pulmonary airspace opacities, more extensive on the left, related to intra-alveolar pulmonary hemorrhage

(ACD/MPV) (Dishop 2011). Pulmonary lymphangiectasia is most often sporadic, but can be associated with genetic disorders, such as Noonan syndrome, yellow nail syndrome, Knobloch syndrome, Urioste syndrome, and mandibulofacial dysostosis. The primary form is typically congenital and may be accompanied by nonimmune hydrops fetalis, congenital chylothorax, or generalized lymphedema (Bellini et al. 2006). Primary pulmonary lymphangiectasia classically presents in a term neonate with severe respiratory distress, tachypnea, cyanosis, and diffuse hazy opacification of the lungs on CXR resembling the findings of surfactant deficiency of prematurity or a genetic disorder of surfactant metabolism. CT reveals smooth septal thickening, bronchovascular bundle thickening, patchy ground-glass opacities, and pleural effusion (Esther and Barker 2004). The pulmonary opacities and septal

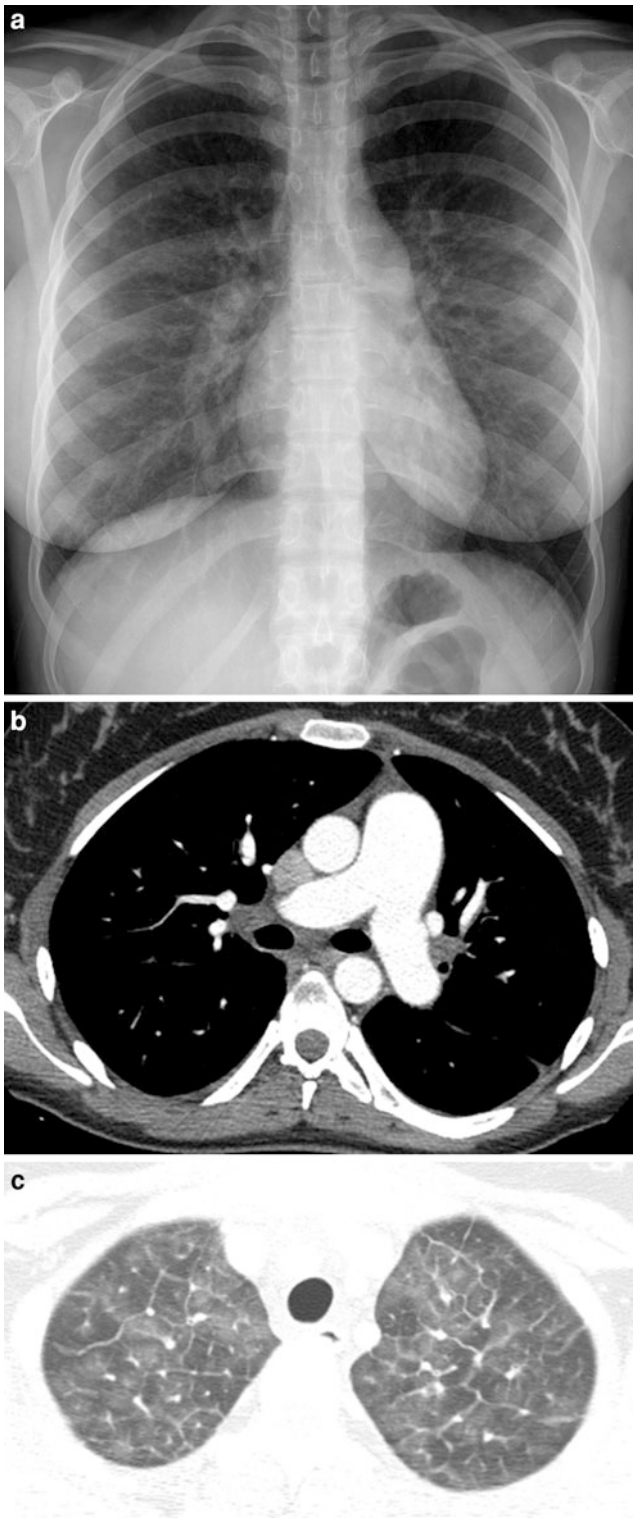

Fig. 22 Pulmonary veno-occlusive disease. A frontal CXR (**a**) of an 18-year-old with progressive dyspnea on exertion shows main pulmonary enlargement and subtle Kerley B lines at the lateral lung bases. Axial chest CT images (**b, c**) confirm the presence of pulmonary artery enlargement and interlobular septal thickening, and reveal mild hilar lymph node enlargement and a tiny pleural effusion

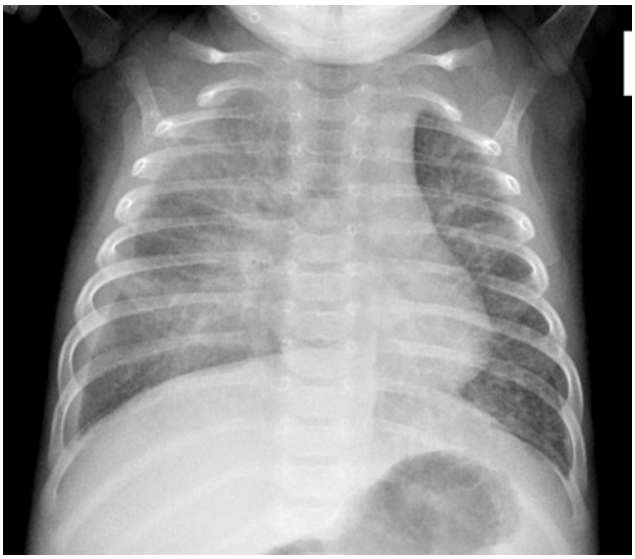

Fig. 23 Pulmonary lymphangiectasia. A frontal CXR of a 2-month-old with a history of congenital chylothorax demonstrates diffuse pulmonary interstitial thickening, pleural effusion, and a normal-sized heart

thickening become less marked, and hyperinflation develops in those surviving infancy or presenting later in childhood (Barker et al. 2004) (Fig. 23). Treatment of primary pulmonary lymphangiectasia is generally supportive, and the overall prognosis is poor (Mettauer et al. 2009).

Pulmonary lymphangiectasia can be confused for lymphangiomatosis. In lymphangiomatosis, there is proliferation of complex anastomosing lymphatic channels with secondary dilation of the lymphatics. Septal thickening, ground-glass opacities and chylous effusions are observed in both lymphangiomatosis and lymphangiectasia. In contrast to lymphangiectasia, lymphangiomatosis tends to present later in childhood and involve extrapulmonary tissues, with lytic bone lesions and mediastinal soft tissue edema being particularly distinctive (Faul et al. 2000; Swenson et al. 1995; Shah et al. 2011). Lymphangiomatosis is further discussed in the chapter entitled Pulmonary and Extrathymic Mediastinal Tumors by Lyons, Guillerman, and McHugh in this book.

3.8 Conclusion

Pediatric DLD comprises a diverse group of disorders with widespread involvement of the pulmonary interstitium, distal airspaces, or peripheral airways resulting in impaired gas exchange and, in some cases, high morbidity and mortality. A novel classification scheme specific for pediatric DLD has been devised, acknowledging the effect of the stage of lung

growth and development on disease manifestations, and incorporating recent insights into the etiology, pathophysiology, genetics, and clinical phenotypes of these disorders, some of which are unique to infants and young children. Familiarity with the classification, clinical presentation, and characteristic imaging features is required for appropriate diagnosis and management of pediatric DLD.

References

Aukland SM, Halvorsen T, Fosse KR, Daltveit AK, Rosendahl K (2006) High-resolution CT of the chest in children and young adults who were born prematurely: findings in a population-based study. AJR Am J Roentgenol 187:1012–1018

Balinotti JE, Chakr VC, Tiller C, Kimmel R, Coates C, Kisling J, Yu Z et al (2010) Growth of lung parenchyma in infants and toddlers with chronic lung disease of infancy. Am J Respir Crit Care Med 181:1093–1907

Bandeira T, Negreiro F, Ferreira R, Salguerio M, Lobo L, Aguiar P, Trindade JC (2011) Clinical, radiological, and physiological differences between obliterative bronchiolitis and problematic severe asthma in adolescents and young adults: the early origins of the overlap syndrome? Pediatr Pulmonol 46:573–580

Barker PM, Esther CR Jr, Fordham LA, Maygarden SJ, Funkhouser WK (2004) Primary pulmonary lymphangiectasia in infancy and childhood. Eur Respir J 24:413–419

Bellini C, Boccardo F, Campisi C, Bonioli E (2006) Congenital pulmonary lymphangiectasia. Orphanet J Rare Diseases 1:43

Bhandari A, Bhandari V (2009) Pitfalls, problems, and progress in bronchopulmonary dysplasia. Pediatrics 123:1562–1573

Biko DM, Schwartz M, Anupindi SA, Altes TA (2008) Subpleural lung cysts in Down syndrome: prevalence and association with coexisting diagnoses. Pediatr Radiol 38:280–284

Bouros D, Nicholson AC, Polychronopoulos V, du Bois RM (2000) Acute interstitial pneumonia. Eur Respir J 15:412–418

Brody AS, Guillerman RP, Hay TC, Wagner BD, Young LR, Deutsch GH, Fan LL et al (2010) Neuroendocrine cell hyperplasia of infancy: diagnosis with high-resolution CT. AJR 194:1–7

Buchvald F, Petersen BL, Damgaard K, Deterding R, Langston C, Fan LL, Deutsch GH et al (2011) Frequency, treatment, and functional outcome in children with hypersensitivity pneumonitis. Pediatr Pulmonol 46:1098–1107

Bullard JE, Nogee LM (2007) Heterozygosity for ABCA3 mutations modifies the severity of lung disease associated with a surfactant protein C gen (SFTPC) mutation. Pediatr Res 62:176–179

Canakis AM, Kutz E, Manson D, O'Brodovich H (2002) Pulmonary interstitial glycogenosis: a new variant of interstitial neonatal lung disease. Am J Respir Crit Care Med 165:1557–1575

Carre A, Szinnai G, Castanet M, Sura-Trueba S, Tron E, Broutin-L'Hermite I, Barat P et al (2009) Fine new TTF1/NKX2.1 mutations in brain-lung-thyroid syndrome: rescue by PAX8 synergism in one case. Hum Mol Genet 18:2266–2276

Castillo M, Vade A, Lim-Dunham JE, Masuda E, Massarani-Wafai R (2010) Pulmonary interstitial glycogenosis in the setting of lung growth abnormality: radiographic and pathologic correlation. Pediatr Radiol 40:1562–1565

Chow CW, Massie J, Ng J, Mills J, Baker M (2013) Acinar dysplasia of the lungs: variation in the extent of involvement and clinical features. Pathology 45:38–43

Clement A, Eber E (2008) Interstitial lung diseases in infants and children. Eur Respir J 31:658–666

Clement A, Nathan N, Epaud R, Fauroux B, Corvol H (2010) Interstitial lung diseases in children. Orphanet J Rare Diseases 5:22

Colom AJ, Teper AM (2009) Clinical prediction rule to diagnose post-infectious bronchiolitis obliterans in children. Pediatr Pulmonol 44:1065–1069

de Wit MC, Tiddens HA, de Coo IF, Mancini GM (2011) Lung disease in FLNA mutation: confirmatory report. Eur J Med Genet 54:299–300

Deterding RR (2010) Infants and young children with children's interstitial lung disease. Pediatr Allerg Immunol Pulmonol 23:25–31

Deterding RR, Pye C, Fan LL, Langston C (2005) Persistent tachypnea of infancy is associated with neuroendocrine cell hyperplasia. Pediatr Pulmonol 40:157–165

Deutsch GH, Young LR (2010) Pulmonary interstitial glycogenosis: words of caution. Pediatr Radiol 40:1471–1475

Deutsch GH, Young LR, Deterding RR, Fan LL, Dell SD, Bean JA, Brody AS et al (2007) Diffuse lung disease in young children: application of a novel classification scheme. Am J Respir Crit Care Med 176:1120–1128

Dishop MK (2010) Diagnostic pathology of diffuse lung disease in children. Pediatr Allergy Immunol Pulmonol 23:69–85

Dishop MK (2011) Paediatric interstitial lung disease: classification and definitions. Paediatr Respir Rev 12:230–237

Doan ML, Guillerman RP, Dishop MK, Nogee LM, Langston C, Mallory GB, Sockrider MM et al (2008) Clinical, radiological and pathological features of ABCA3 mutations in children. Thorax 63:366–373

Ehsan Z, Montgomery GS, Tiller C, Kisling J, Chang DV, Tepper RS (2014) An infant with pulmonary interstitial glycogenosis: clinical improvement is associated with improvement in the pulmonary diffusion capacity. Pediatr Pulmonol 49:E17–E20

Esther CR Jr, Barker PM (2004) Pulmonary lymphangiectasia: diagnosis and clinical course. Pediatr Pulmonol 38:308–313

Fan LL, Deterding RR, Langston C (2004) Pediatric interstitial lung disease revisited. Pediatr. Pulmunol 38:369–378

Faul JL, Berry GJ, Colby TV, Ruoss SJ, Walter MB, Rosen GD, Raffin TA (2000) Thoracic lymphangiomas, lymphangiectasis, lymphangiomatosis, and lymphatic dysplasia syndrome. Am J Respir Crit Care Med 161:1037–10460

Flamein F, Riffault L, Muselet-Charlier C, Pernelle J, Feldmann D, Jonard L, Durand-Schneider AM et al (2012) Molecular and cellular characteristics of ABCA3 mutations associated with diffuse parenchymal lung diseases in children. Hum Mol Genet 21:765–775

Frazier AA, Franks TJ, Mohammed TL, Ozbudak IH, Galvin JR (2007) From the archives of the AFIP: pulmonary veno-occlusive disease and pulmonary capillary hemangiomatosis. Radiographics 27:867–882

Galambos C, Levy H, Cannon CL, Vargas SO, Reid LM, Cleveland R, Lindeman R et al (2010) Pulmonary pathology in thyroid transcription factor-1 deficiency syndrome. Am J Respir Crit Care Med 182:549–554

Galambos C, Sims-Lucas S, Abman SH (2014) Three-dimensional reconstruction identifies misaligned pulmonary veins as intrapulmonary shunt vessels in alveolar capillary dysplasia. J Pediatr 164:192–195

Gendelman S, Zeft A, Spalding SJ (2013) Childhood-onset eosinophilic granulomatosis with polyangiitis (formerly Churg-Strauss syndrome): a contemporary single-center cohort. J Rheumatol 40:929–935

Gillespie LM, Fenton AC, Wright C (2004) Acinar dysplasia: a rare cause of neonatal respiratory failure. Acta Paediatr 93:712–713

Giovannini-Chami L, Hadchouel A, Nathan N, Bremont F, Dubus J-C, Fayon M, Houdouin V et al (2014) Idiopathic eosinophilic pneumonia in children: the French experience. Orphanet J Rare Diseases 9:28

Gomes VC, Silva MC, Maia JH, Daltro P, Ramos SG, Brody AS, Marchiori E (2013) Diagnostic criteria and follow-up in neuroendocrine cell hyperplasia of infancy: a case series. J Bras Pnumol 39:569–578

Guillerman RP (2010) Imaging of childhood interstitial lung disease. Pediatr Allerg Immunol Pulmonol 23:43–68

Guillerman RP, Brody AS (2011) Contemporary perspectives on pediatric diffuse lung disease. Radiol Clin N Am 49:847–868

Guillerman RP, Metwalli ZA, Burrage LC, Lalani SR, Langston C, Mallory GB (2013) Congenital multilobar pseudo-emphysema: a severe progressive lung growth disorder associated with filamin A gene mutations. Pediatr Radiol 43:S304 (Suppl 2)

Guillot L, Epaud R, Thouvenin G, Jonard L, Mohsni A, Couderc R, Counil F et al (2009) New surfactant protein C gene mutations associated with diffuse lung disease. J Med Genet 46:490–494

Guillot L, Carre A, Szinnai G, Castanet M, Tron E, Jaubert F, Broutin I et al (2010) NKX2-1 mutations leading to surfactant protein promoter dysregulation cause interstitial lung disease in "brain-lung-thyroid" syndrome. Hum Mutat 31:E1146–E1162

Hamvas A (2010) Evaluation and management of inherited disorders of surfactant metabolism. Chin Med J (Engl) 123:2943–2947

Hamvas A, Deterding RR, Wert SE, White FV, Dishop MK, Alfano DN, Halbower AC et al (2013) Heterogeneous pulmonary phenotypes associated with mutations in the thyroid transcription factor gene NKX2-1. Chest 144:794–804

Hartman TE (2003) The HRCT features of extrinsic allergic alveolitis. Semin Respir Crit Care Med 24:419–426

Hendrickx GF, Somers K, Vandenplas Y (2011) Lane-Hamilton syndrome: case report and review of the literature. Eur J Pediatr 170:1597–1602

Hoepker A, Seear M, Petrocheilou A, Hayes D Jr, Nair A, Deodhar J, Kadam S, O'Toole J (2008) Wilson-Mikity syndrome: updated diagnostic criteria based on nine cases and a review of the literature. Pediatr Pulmonol 43:1004–1012

Hoganson DM, Gazit AZ, Boston US, Sweet SC, Grady RM, Huddleston CB, Eghtesady P (2014) Paracorporeal lung assist devices as a bridge to recovery of lung transplantation in neonates and young children. J Thorac Cardiovasc Surg 147:420–426

Hugosson CO, Salama HM, Al-Dayel F, Khoumais N, Kattan AH (2005) Primary alveolar capillary dysplasia (acinar dysplasia) and surfactant protein B deficiency: a clinical, radiological and pathological study. Pediatr Radiol 35:311–316

Jeong YJ, Kim KI, Seo IJ, Lee CH, Lee KN, Kim KN, Kim JS et al (2007) Eosinophilic lung diseases: a clinical, radiologic, and pathologic overview. Radiographics 27:617–637

Kerby GS, Wagner BD, Popler J, Hay TC, Kopecky C, Wilcox SL, Quinones RR et al (2013) Abnormal infant pulmonary function in young children with neuroendocrine cell hyperplasia of infancy. Pediatric Pulmonol 48:1008–1015

King BA, Boyd JT, Kingma PS (2011) Pulmonary maturation arrest and death in a patient with pulmonary interstitial glycogenosis. Pediatr Pulmonol 46:1142–1145

Kjellberg M, Bjorkman K, Rohdin M, Sanchez-Crespo A, Jonsson B (2013) Bronchopulmonary dysplasia: clinical grading in relation to ventilation/perfusion mismatch measured by single photon emission computed tomography. Pediatr Pulmonol 48:1206–1213

Kligerman SJ, Groshong S, Brown KK, Lynch DA (2009) Nonspecific interstitial pneumonia: radiologic, clinical, and pathologic considerations. Radiographics 29:73–87

Kligerman SJ, Franks TJ, Galvin JR (2013) From the radiologic pathology archives: organization and fibrosis as a response to lung injury in diffuse alveolar damage, organizing pneumonia, and acute fibrinous and organizing pneumonia. Radiographics 33:1951–1975

Kradin RL, Mark EJ (2008) The pathology of pulmonary disorders due to Aspergillus spp. Arch Pathol Lab Med 132:606–614

Kurland G, Deterding RR, Hagood JS, Young LR, Brody AS, Castile RG, Dell S et al (2013) An official American Thoracic Society clinical practice guideline: classification, evaluation and management of childhood interstitial lung disease in infancy. Am J Respir Crit Care Med 188:376–394

la Tour T, Spadola L, Sayegh Y, Combescure C, Pfister R, Argiroffo CB, Rochat I (2013) Chest CT in bronchopulmonary dysplasia: clinical and radiological correlations. Pediatr Pulmonol 48:693–698

Lanfranchi M, Allbery SM, Wheelock L (2010) Pulmonary interstitial glycogenosis. Pediatr Radiol 40:361–365

Langston C, Dishop MK (2009) Diffuse lung disease in infancy: a proposed classification scheme applied to 259 diagnostic biopsies. Pediatr Dev Pathol 12:421–437

Lee EY (2013) Interstitial lung disease in infants: new classification system, imaging technique, clinical presentation and imaging findings. Pediatr Radiol 43:3–13

Lino CA, Batista AK, Soares MA, de Freitas AE, Gomes LC, M Filho JH, Gomes VC (2013) Bronchiolitis obliterans: clinical and radiological profile of children follow-up in a reference clinic. Rev Paul Pediatr 31:10–16

Liu XY, Jiang ZF, Zhou CJ, Peng Y (2011) Clinical features of 3 cases with acute interstitial pneumonia in children. Zhoghua Er Ke Za Zhi 49:98–102

Lucaya J, Gartner S, García-Peña P, Cobos N, Roca I, Liñan S (1998) Spectrum of manifestations of Swyer-James-MacLeod syndrome. J Comput Assist Tomogr 22:592–597

Lukkarinen K, Pelkonen A, Lohi J, Malmstrom K, Malmberg LK, Kajosaari M, Lindahl H et al (2013) Neuroendocrine cell hyperplasia of infancy: a prospective follow-up of nine children. Arch Dis Child 98:141–144

MacDonald S, Müller NL (2003) Insights from HRCT: how they affect the management of diffuse parenchymal lung disease. Semin Respir Crit Care Med 24:357–364

Mahut B, de Blic J, Emond S, Benoist MR, Jarreau PH, Lacaze-Masmonteil T, Magny JF et al (2007) Chest computed tomography findings in bronchopulmonary dysplasia and correlation with lung function. Arch Dis Child Fetal Neonatal Ed 92:F459–F464

Marchiori E, Zanetti G, Mano CM, Irion KL, Daltro PA, Hochhegger B (2010) Lipoid pneumonia in 53 patients after aspiration of mineral oil: comparison of high-resolution computed tomography findings in adults and children. J Comput Assist Tomogr 34:9–12

Martinez-Moczygemba M, Doan ML, Elidemir O, Fan LL, Cheung SW, Lei JT, Moore JP et al (2008) Pulmonary alveolar proteinosis caused by deletion of the GM-CSFRα gene in the X chromosome pseudoautosomal region 1. J Exp Med 205:2711–2716

Masurel-Paulet A, Haan E, Thompson EM, Goizet C, Thauvin-Robinet C, Tai A, Kennedy A et al (2011) Lung disease associated with periventricular nodular heterotopia and an FLNA mutation. Eur J Med Genet 54:25–28

Mattiello R, Sarria EE, Mallol J, Fischer GB, Mocelin H, Bello R, Flores JA et al (2010) Post-infectious bronchiolitis obliterans: can CT scan findings at early age anticipate lung function? Pediatr Pulmonol 45:315–319

Mechri M, Epaud R, Emond S, Coulomb A, Jaubert F, Tarrant A, Feldmann D et al (2010) Surfactant protein C gene (SFTPC) mutation-associated lung disease: high-resolution computed tomography (HRCT) findings and its relation to histological analysis. Pediatr Pulmonol 45:1021–1029

Mettauer N, Agrawal S, Pierce C, Ashworth M, Petros A (2009) Outcome of children with pulmonary lymphangiectasis. Pediatr Pulmonol 44:351–357

Metwalli ZA, Guillerman RP, Langston C (2011) Alveolar growth abnormalities: not just BPD. Pediatr Radiol 41:S250 (Suppl 1)

Michalsky MP, Arca MJ, Groenman F, Hammond S, Tibboel D, Caniano DA (2005) Alveolar capillary dysplasia: a logical approach to a fatal disease. J Pediatr Surg 40:1100–1105

Moissidis I, Chaidaroon D, Vichyanond P, Bahna SL (2005) Milk-induced pulmonary disease in infants (Heiner syndrome). Pediatr Allergy Immunol 16:545–552

Montani D, Price LC, Dorfmuller P, Achouh L, Jais X, Yaici A, Sitbon O et al (2009) Pulmonary veno-occlusive disease. Eur Respir J 33:189–200

Moonnumakal SP, Fan LL (2008) Bronchiolitis obliterans in children. Curr Opin Pediatr 20:272–278

Narayanan M, Owers-Bradley J, Beardsmore CS, Mada M, Ball I, Garipov R, Panesar KS et al (2012) Alveolarization continues during childhood and adolescence. New evidence from helium-3 magnetic resonance. Am J Respir Crit Care Med 185:186–191

Nathan N, Taam RA, Epaud R, Delacourt C, Deschildre A, Reix P, Chiron R et al (2012) A national internet-linked based database for pediatric interstitial lung diseases: the French network. Orphanet J Rare Diseases 7:40

Newman B, Yunis E (1990) Primary alveolar capillary dysplasia. Pediatr Radiol 21:20–22

Nogee LM (2006) Genetics of pediatric interstitial lung disease. Curr Opin Pediatr 18:287–292

Nogee LM (2010) Genetic basis of children's interstitial lung disease (chILD). Pediatr Allerg Immunol Pulmonol 23:15–24

Oermann CM, Panesar KS, Langston C, Larsen GL, Menendez AA, Schofield DE, Cosio C et al (2000) Pulmonary infiltrates with eosinophilia syndromes in children. J Pediatr 136:351–358

Ogier de Baulny H, Schiff M, Dionisi-Vici C (2012) Lysinuric protein intolerance (LPI): a multi organ disease by far more complex than a classic urea cycle disorder. Mol Genet Metab 106:12–17

Olsen ØE, Sebire NJ, Jaffe A, Owens CM (2004) Chronic pneumonitis of infancy: high-resolution CT findings. Pediatr Radiol 34:86–88

Onland W, Molenaar JJ, Leguit RJ, van Nierop JC, Noorduyn LA, van Rijn RR, Geukers VG (2005) Pulmonary interstitial glycogenosis in identical twins. Pediatr Pulmonol 40:362–366

Parto K, Svedström E, Majurin ML, Harkonen R, Simell O (1993) Pulmonary manifestations in lysinuric protein intolerance. Chest 104:1176–1182

Philip AG (2009) Chronic lung disease of prematurity: a short history. Semin Fetal Neonatal Med 14:333–338

Polverosi R, Maffesanti M, Dalpiaz G (2006) Organizing pneumonia: typical and atypical HRCT patterns. Radiol Med 111:202–212

Popler J, Gower WA, Mogayzel PJ Jr, Nogee LM, Langston C, Wilson AC, Hay TC et al (2010) Familial neuroendocrine cell hyperplasia of infancy. Pediatr Pulmonol 45:749–755

Popler J, Lesnick B, Dishop MK, Deterding RR (2012) New coding in the International Classification of Diseases, ninth revision, for children's interstitial lung disease. Chest 142:774–780

Prestridge A, Wooldridge J, Deutsch G, Young LR, Wert SE, Whitsett JA, Nogee L (2006) Persistent tachypnea and hypoxia in a 3-month-old term infant. J Pediatr 149:702–706

Radman MR, Goldhoff P, Jones KD, Azakie A, Datar S, Adatia I, Oishi PE, Fineman JR (2013) Pulmonary interstitial glycogenosis: an unrecognized etiology of persistent pulmonary hypertension of the newborn in congenital heart disease? Pediatr Cardiol 34:1254–1257

Rice A, Tran-Dang M-A, Bush A, Nicholson AG (2013) Diffuse lung disease in infancy and childhood: expanding the chILD classification. Histopathology 63:743–755

Robinson TE, Trapnell BC, Goris ML, Quitell LM, Cornfield DN (2009) Quantitative analysis of longitudinal response to aerosolized granulocyte-macrophage colony-stimulating factor in two adolescents with autoimmune pulmonary alveolar proteinosis. Chest 135:842–848

Santamaria F, Parenti G, Guidi G, Rotondo A, Grillo G, Larocca MR, Celentano L et al (1996) Early detection of lung involvement in lysinuric protein intolerance: role of high-resolution computed tomography and radioisotopic methods. Am J Respir Crit Care Med 153:731–735

Sarria EE, Mattiello R, Rao L, Wanner MR, Raske ME, Tiller C, Kimmel R, Tepper RS (2011) Computed tomography score and pulmonary function in infants with chronic lung disease of infancy. Eur Respir J 38:918–923

Sen P, Thakur N, Stockton DW, Langton C, Bejjani BA (2004) Expanding the phenotype of alveolar capillary dysplasia. J Pediatr 145:646–651

Sen P, Yang Y, Navarro C, Silva I, Szafranski P, Kolodziejska KE, Dharmadhikari AV et al (2013) Novel FOXF1 mutations in sporadic and familial cases of alveolar capillary dysplasia with misaligned pulmonary veins imply a role for its DNA binding domain. Hum Mutat 34:801–811

Shah V, Shah S, Barnacle A, Sebire NJ, Brock P, Harper JI, McHugh K et al (2011) Mediastinal involvement in lymphangiomatosis: a previously unreported. Pediatr Radiol 41:985–992

Shin S-M, Kim WS, Cheon J-E, Kim HS, Lee W, Jung AY, Kim I-O, Choi JH (2013) Bronchopulmonary dysplasia: new high resolution computed tomography scoring system and correlation between the high resolution computed tomography score and clinical severity. Korean J Radiol 14:350–360

Smets K, Dhaene K, Schelstraete P, Meersschaut V, Vanhaesebrouk P (2004) Neonatal pulmonary interstitial glycogen accumulation disorder. Eur J Pediatr 163:408–409

Smith KJ, Dishop MK, Fan LL, Moonnumakal SP, Smith EO, Bayindir P, Guillerman RP (2011) Diagnosis of bronchiolitis obliterans with computed tomography in children. Pediatr Allerg Immunol Pulmonol 23:253–259

Soares JJ, Deutsch GH, Moore PE, Fazili MF, Austin ED, Brown RF, Sokolow AG et al (2013) Childhood interstitial lung diseases: an 18-year retrospective analysis. Pediatrics 132:684

Soraisham AS, Tierney AJ, Amin HJ (2006) Neonatal respiratory failure associated with mutation in the surfactant protein C gene. J Perinatol 26:67–70

Stankiewicz P, Sen P, Bhatt SS, Storer M, Xia Z, Bejjani BA, Ou Z et al (2009) Genomic and genic deletions of the FOX gene cluster on 16q24.1 and inactivating mutations of FOXF1 cause alveolar capillary dysplasia and other malformations. Am J Hum Genet 84:780–791

Stevens PA, Pettenazzo A, Brasch F, Mulugeta S, Baritussio A, Ochs M, Morrison L et al (2005) Nonspecific interstitial pneumonia, alveolar proteinosis, and abnormal proprotein trafficking resulting from a spontaneous mutation in the surfactant protein C gene. Pediatr Res 57:89–98

Suzuki T, Sakagami T, Rubin BK, Nogee LM, Wood RE, Zimmerman SL, Smolarek T et al (2008) Familial pulmonary alveolar proteinosis caused by mutations in *CSF2RA*. J Exp Med 205:2703–2710

Suzuki T, Sakagami T, Young LR, Carey BC, Wood RE, Luisetti M, Wert SE et al (2010) Hereditary pulmonary alveolar proteinosis: pathogenesis, presentation, diagnosis, and therapy. Am J Respir Crit Care Med 182:1292–1304

Swenson SJ, Hartman TE, Mayo JR, Colby TV, Tazelaar HD, Muller NL (1995) Diffuse pulmonary lymphangiomatosis: CT findings. J Comput Assist Tomogr 19:348–352

Taytard J, Nathan N, de Blic J, Fayon M, Epaud R, Deschildre A, Troussier J et al (2013) New insights into pediatric idiopathic pulmonary hemosiderosis: the French RespiRare Cohort. Orphanet J Rare Diseases 8:161

Thouvenin G, Taam RA, Flamein F, Guillot L, le Bourgeois M, Reix P, Fayon M et al (2010) Characteristics of disorders associated with genetic mutations of surfactant protein C. Arch Dis Child 95:449–454

Travis WD, Hunninghake G, King TE Jr, Lynch DA, Colby TV, Galvin JR, Brown KK et al (2008) Idiopathic nonspecific interstitial pneumonia: report of an American Thoracic Society project. Am J Respir Crit Care Med 177:1338–1347

Travis WD, Costabel U, Hansell DM, King TE Jr, Lynch DA, Nicholson AG, Ryerson CJ et al (2013) An official American Thoracic Society/European Respiratory Society statement: update of the international multidisciplinary classification of the idiopathic interstitial pneumonias. Am J Respir Crit Care Med 188: 733–748

Vece TJ, Fan LL (2010) Interstitial lung disease in children older than 2 years. Pediatr Allerg Immunol Pulmonol 23:33–41

Vece TJ, Fan LL (2011) Diagnosis and management of diffuse lung disease in children. Paediatr Respir Rev 12:238–242

Wambach JA, Wegner DJ, Depass K, Heins H, Druley TE, Mitra RD, An P et al (2012) Single ABCA3 mutations increase the risk for neonatal respiratory distress syndrome. Pediatrics 130:e1575–e1582

Woerner C, Cutz E, Yoo S-J, Grasemann H, Humpl T (2014) Pulmonary veno-occlusive disease in childhood. Chest. doi: 10.1378/chest.13-0172 (Epub ahead of print)

Wong PM, Lees AN, Louw J, Lee FY, French N, Gain K, Murray CP, Wilson A, Chambers DC (2008) Emphysema in young adult survivors of moderate-to-severe bronchopulmonary dysplasia. Eur Respir J 32:321–328

Wong P, Murray C, Louw J, French N, Chambers D (2011) Adult bronchopulmonary dysplasia: computed tomography findings. J Med Imaging Radiat Oncol 55:373–378

Yalcin E, Dog D, Haliloglu M, Ozcelik U, Kiper N, Gocmen A (2003) Postinfectious bronchiolitis obliterans in children: clinical and radiological profile and prognostic factors. Respiration 70:371–375

Young LR, Brody AS, Inge TH, Acton JD, Bokulic RE, Langston C, Deutsch GH (2010) Neuroendocrine cell distribution and frequency distinguish neuroendocrine cell hyperplasia of infancy from other pulmonary disorders. Chest 139:1060–1071

Young LR, Deutsch GH, Bokulic RE, Brody AS, Nogee LM (2013) A mutation in TTF1/NKX2.1 is associated with familial neuroendocrine cell hyperplasia of infancy. Chest 144:1199–1206

Zanetti G, Marchiori E, Gasparetto TD, Escuissato DL, Soares Souza A Jr (2007) Lipoid pneumonia in children following aspiration of mineral oil used in the treatment of constipation: high-resolution CT findings in 17 patients. Pediatr Radiol 37:1135–1139

Zhang L, Irion K, da Silva Porto N, Abreu e Silva F (1999) High-resolution computed tomography in pediatric patients with post-infectious bronchiolitis obliterans. J Thorac Imaging 14:85–89